Tracking centennial changes in algal community composition and biomass using subfossil pigments in a high mountain lake (Sierra Nevada, Spain).

Joana Llodrà-Llabrés[1,#], Carmen Pérez-Martínez[1,#], Teresa Vegas-Vilarrúbia[2], John P. Smol[3], Carsten Meyer-Jacob[4], Javier Sigro[5], Teresa Buchaca[6]

[1]Department of Ecology and Institute for Water Research, University of Granada, 18071 Granada, Spain
[2]Department of Evolutionary Biology, Ecology and Environmental Sciences, Universitat de Barcelona, Av. Diagonal 643, 08028 Barcelona, Spain
[3]Paleoecological Environmental Assessment and Research Laboratory, Department of Biology, Queen's University, Kingston, Ontario K7L 3N6, Canada
[4]Université du Québec en Abitibi-Témiscamingue. Institut de Recherche sur les Forêts (IRF) 445 Boulevard de l'Université, Rouyn-Noranda, QC, J9X 5E4, Canada
[5]Centre for Climatic Change (C3), Research Institute in Sustainability, Climate Change and Energy Transition, University Rovira i Virgili, C. Joanot Martorell 15, 43480 Vilaseca, Tarragona, Spain
[6]Integrative Freshwater Ecology (CEAB-CSIC), C/ Accés a la Cala St. Francesc, 14, 17300, Blanes, Girona, Spain

[#]These authors contributed equally to this work

Correspondence to: Carmen Pérez-Martínez (cperezm@ugr.es)

Abstract. Remote aquatic ecosystems are affected by the rapid intensification of human-driven climate change, along with increasing atmospheric nutrient deposition. However, there is a lack of studies that examine changes in the composition of the overall algal community, including cyanobacteria, over extended periods of time. This study investigates shifts in pigment assemblage composition and algal community biomass over approximately the past 430 years. We used high-resolution (2.5 mm intervals), well-dated sediment core from Borreguil Lake, a high-altitude lake in the Sierra Nevada Mountains (Southern Spain). We noted a significant change in both algal biomass and community composition throughout the core, with a notable intensification since the ca. 1970s, which appears to be linked to increasing temperatures and aerosol deposition. Algal biomass and composition exhibited two significant shifts approximately between 1740–1840 and from 1970 to the present, with the latter period reaching unprecedented increases in algal biomass. From the bottom to the top, the compositional shifts were characterized by an increase in cyanobacteria (indicated by aphanizophyll and scytonemin), cryptophytes (indicated by alloxanthin), and green algae (indicated by lutein and zeaxanthin), at the expense of diatoms (indicated by diatoxanthin).

Statistical analyses revealed that both algal biomass and composition were strongly influenced by warming temperatures, reduced precipitation, and enhanced Saharan dust deposition. In particular, the increase in nitrogen-fixing cyanobacteria (indicated by aphanizophyll) since the 1970s has led to previously unrecorded nitrogen fixation in the lake. This is probably due to reduced nitrogen availability compared to phosphorus, which is brought disproportionally to this lake by Saharan dust. The observed changes in the algal community in Borreguil Lake are unprecedented in the last ~400 years in the Sierra Nevada lakes and were temporally related to algal community shifts in other Mediterranean sites suggesting that rising global temperatures, aerosol deposition and enhanced Saharan dust deposition will likely continue to affect the ecological condition of these ecosystems. Projected increases in global temperatures and Saharan dust deposition will likely lead to an increase in the lake trophic status and significant changes in algal composition in Borreguil Lake.

1 Introduction

High mountain lakes are especially vulnerable to climate warming (Moser et al., 2019; Sorvari and Korhola, 1998). Their physical constraints, nutrient limitations, and inherently low productivity and biodiversity amplify the effects of environmental change. Furthermore, stressors linked to climate warming, such as rising temperatures, are often intensified in these ecosystems (Pepin et al., 2015). As a result, these remote lakes are considered biospheric sentinels of global change (Adrian et al., 2009). In addition to changes caused by climate warming, remote lakes are sometimes exposed to increased atmospheric nitrogen deposition due to human activities (Bergström and Jansson, 2006). Recent evidence further indicates that phosphorus deposition in alpine ecosystems is increasing (Brahney et al., 2014; Camarero and Catalán, 2012; Jiménez et al., 2018), mainly due to windblown dust from distant phosphorus sources.

Of particular concern is the case of high mountain lakes in the Mediterranean region, as they face two distinct forms of stress: intensification of climate warming because their high-altitude location and intensification of summer droughts because of their position within the Mediterranean zone (Nogués-Bravo et al., 2008). Projections for the Mediterranean region indicate substantial temperature increases and precipitation decreases (IPCC, 2022; López-Merino et al., 2011). Climate models predict that regional warming will occur at rates 20% higher than the global average, along with a 12% reduction in precipitation under a scenario of 3°C global temperature rise. As a result, the region is considered a critical 'hotspot' in future climate projections (Giorgi, 2006; IPCC, 2022). Additionally, significant amounts of Saharan dust are regularly transported to the Mediterranean Basin (Salvador et al., 2022), delivering key nutrients, such as calcium, phosphorus and iron the Mediterranean ecosystems.

This study has been conducted in the Sierra Nevada range (Southern Spain), which is the highest range in the Iberian Peninsula and southern Europe and contains around 50 small, shallow lakes with remote locations, minimal human impact, low primary production, and low alkalinity (Medina-Sánchez et al., 2022). Despite the well-documented impacts of climate change on Sierra Nevada high mountain lakes, the long-term response of algal community composition remains unknown. In this study,

we analyse changes in algal biomass and community composition over the last 430 years in Borreguil Lake by examining sedimentary pigment concentrations. Whereas many previous studies have addressed changes in a particular group of organisms (e.g. diatoms or cladocerans) during the Industrial Era, we focus on an in-depth analysis of shifts in the algal community and adopt a relatively longer timescale, expanding our scope back to the Little Ice Age (LIA).

Several paleolimnological studies conducted in Sierra Nevada lakes focus on the Anthropocene period (last ~200 years) and suggest that rising regional air temperatures, reduced precipitation, and increased phosphorus and calcium-rich Saharan dust deposition are the primary drivers of ecological changes observed in six Sierra Nevada lakes (Pérez-Martínez et al., 2022). Notably, these climate changes have increased chlorophyll-*a* concentrations, with more pronounced effects since the ~1970s yr CE and have influenced diatom (Pérez-Martínez et al., 2020b) and cladoceran assemblages (Jiménez et al., 2018). Additionally, shifts in chironomid assemblages in Río Seco Lake (Sierra Nevada) are also driven by increasing temperatures (Jiménez et al., 2019). Moreover, previous limnological studies within the Sierra Nevada region have elucidated the impacts of interannual climatic variations, including temperature, rainfall, and Saharan dust deposition, on biogeochemical processes and lake biota (Morales-Baquero et al., 2006a, b; Pérez-Martínez et al., 2007). However, the long-term response of algal community composition (i.e. since the LIA) remains unknown.

Here, we provide detailed analyses of sedimentary pigments, in addition to other biogeochemical indicators such as stable isotopes and the elemental composition of organic matter, from the Little Ice Age to the present (last ~430 years). Pigment-based methods allow for the reconstruction of taxonomic group abundances that lack preserved morphological remains (Leavitt and Hodgson, 2001). Accordingly, source-specific sedimentary pigments have been used to identify particular algal groups (Zhang et al., 2019), based on the premise that each algal class has a characteristic pigment composition (Mackey et al., 1996). Pigments have proven to be effective taxonomic markers for studying algal communities in both marine (Riegman and Kraay, 2001) and freshwater ecosystems, including eutrophic and oligotrophic lakes (Buchaca et al., 2005; Oleksy et al., 2020; Schlüter et al., 2006; Tuccillo et al., 2025; Zeng et al., 2025). In remote lakes, sedimentary pigments have been used to link increases in primary production to a variety of environmental drivers, including climate warming (Battarbee et al., 2002; Lami et al., 2010; Michelutti et al., 2005; Michelutti and Smol, 2016) and atmospheric phosphorus inputs (Brahney et al., 2015a).

Based on the information outlined above, we hypothesized that recent climate changes—specifically, rising temperatures and decreasing precipitation in the Sierra Nevada—together with increased phosphorus Saharan dust deposition, have significantly affected the abundance and composition of primary producers in Borreguil Lake, as recorded in sedimentary pigments. We expect that atmospheric input of Saharan-derived phosphorus (P) is particularly relevant given the naturally low levels of this nutrient in the lake (Jiménez et al., 2018; Pérez-Martínez et al., 2020a). Finally, we also extended the study with the analysis of paleoenvironmental proxies such as Carbon:Nitrogen ratio of the sedimentary organic matter (C/N) and added the analysis of new variables such as $\delta^{15}N$ and Dissolved Organic Carbon in lake water (DOCw). In contrast to other studies (Jiménez et al., 2018, Pérez-Martínez et al, 2020a), this study uses climate series obtained specifically for Sierra Nevada summits by Sigro et al. (2024), whereas in previous studies, we used climate series from sites near the Sierra Nevada. Accordingly, we posed

the following research questions: (1) A previous study of the last 180 years shows a significant increase in algal biomass over the last 50 years. Is this increase also significant when viewed over the extended period of 430 years? (2) Has the composition of the algal community shifted over this interval? Overall, this research contributes to a deeper understanding of long-term ecological dynamics in alpine lake algal communities in the context of ongoing climatic and atmospheric changes.

2. Methodology

2.1 Study area

The Sierra Nevada range (Granada, SE Spain) (36° 55′-37° 15′ N, 2° 31′-3° 40′ W) reaches a maximum elevation of 3482 m asl. The summits experience a high-elevation Mediterranean climate, characterized by warm, dry, and ice-free conditions from June to October. The meteorological station at 2507 m asl reports an annual mean temperature of 4.4°C and 700 mm of precipitation, 80% of which falls as snow between October and April. Sierra Nevada lies between European and African biogeographic regions, about 60 km from the coast, and experiences a semi-arid Mediterranean climate (Zamora and Oliva, 2022). Since 1864 CE, the Sierra Nevada region has warmed by 1.56 °C (0.12 °C/decade) mainly due to increase spring and summer temperature (Sigro et al., 2024). Summer precipitation has declined, particularly from 1975 to 2020 CE (-13.4% per decade^{-1}) (Sigro et al., 2024). Sierra Nevada hosts approximately 50 small glacial lakes at elevations of 2800–3100 m asl, formed during the glacial retreat after the last glacial cycle (Castillo Martín, 2009). The geologic substrate in lake catchment basins is composed of slow-weathering, metamorphosed siliceous bedrock mainly mica-schist with graphite and mica-schist with feldspar, devoid of carbonated rocks. These lakes are typically oligotrophic or oligo-mesotrophic, characterized by cold, oxygen-rich waters with low alkalinity and mineralization (Medina-Sánchez et al., 2022). Due to its proximity to Africa, Sierra Nevada lakes are ideal for studying Saharan input effects, as southeastern Iberia is frequently exposed to Saharan dust intrusions (Morales-Baquero and Pérez-Martínez, 2016; Pulido-Villena et al., 2006) and Saharan dust fertilizes in phosphorus, calcium, and alkalizing minerals the oligotrophic lakes that receive it (Morales-Baquero et al., 2006b). Saharan dust deposition has significantly increased in recent decades (Moulin and Chiapello, 2006; Mulitza et al., 2010; Prospero and Lamb, 2003), further influencing ecosystem chemistry and dynamics.

This study focuses on Borreguil Lake (Fig. 1), an oligo-mesotrophic lake at 2980 m asl (37° 03′ 09.53” N, 3° 17′ 59.03” W) with a maximum depth of 2.8 m and an area of 0.18 ha (Supplementary Table S1). The lake is surrounded by approximately 0.56 ha of alpine meadows, the flora of which is mainly composed of Cyperaceae, Poaceae and Fabaceae, with frequent genera including *Carex, Nardus*, *Festuca* and *Scorzoneroides* (Pérez-Luque et al., 2015). The wetter meadow shows bryophyte species such as *Drepanocladus fluitans*. The lake freezes annually from October to May, with interannual variability. It is fishless and does not thermally stratify in summer. The lake basin shows permanent inlets and outlets supplying water during the ice-free period. Physicochemical data are available in Jiménez et al. (2018) and Pérez-Martínez et al. (2020b).

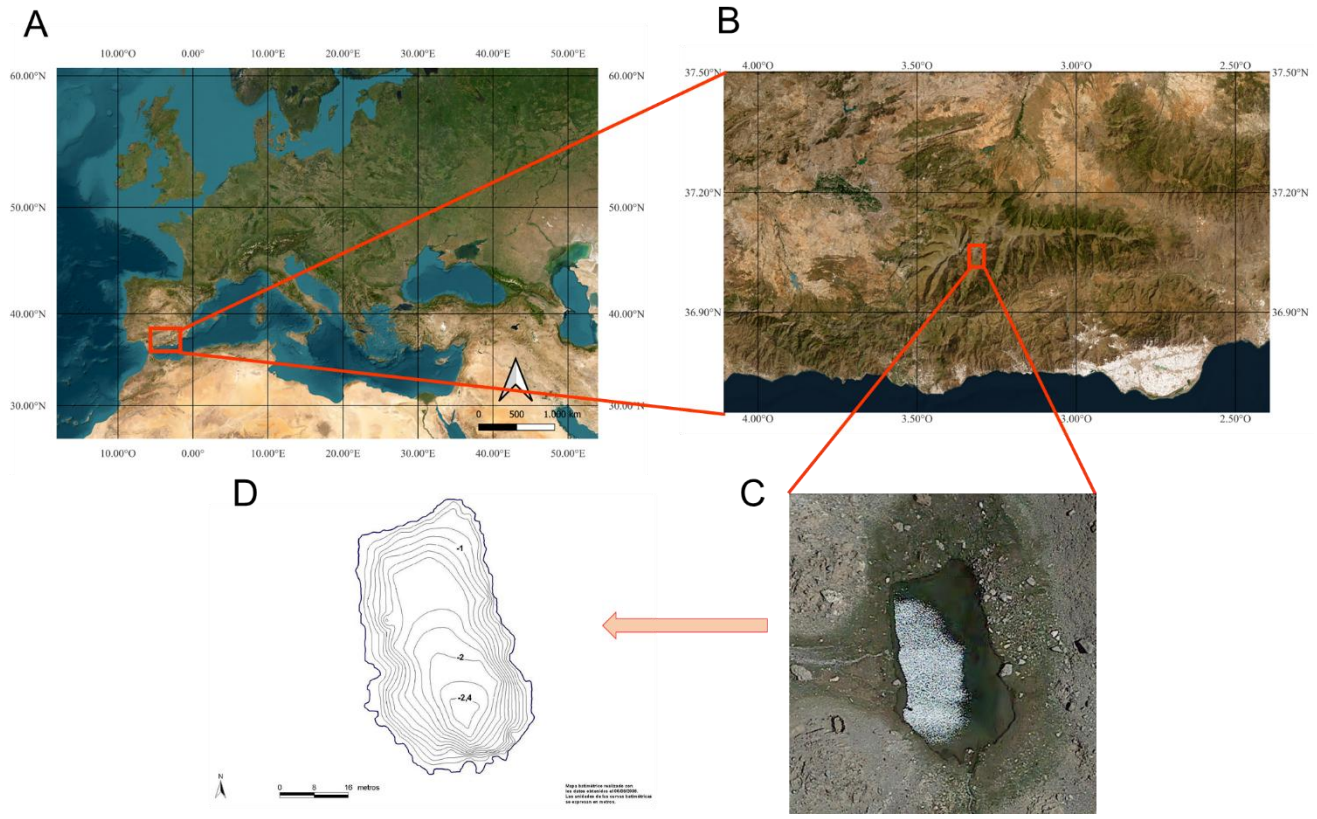

Figure 1: A) Location of Borreguil Lake, Sierra Nevada, Spain. A) Location of Sierra Nevada in southern Spain; B) Location of Borreguil Lake in the range; C) Borreguil Lake; D) Bathymetric map of the lake (extracted from digitized map of bathymetry report from Egmasa S.A.) The orange dot indicates the point at which the sediment core was retrieved. Maps data © Google Earth 2019; Image Landsat/Copernicus.

2.2 Algal community composition of Borreguil Lake

To determine the composition of the phytoplankton, several water column samples were taken at the deepest zone in Borreguil Lake. Phytoplankton (100 mL) was collected from a homogenized volume of water sampled with a tube sampler. Phytoplankton samples were immediately fixed in acetic Lugol's solution and the algae species were identified and counted using an inverted microscope following the Utermöhl technique. The planktonic algal community of Borreguil Lake currently consists of four classes, dominated by Chlorophyceae and Cyanobacteria, followed by Chrysophyceae and Cryptophyceae (Supplementary Fig. S1). Chlorophyceae is the most diverse group, with 17 taxa. Most of the diatoms are periphytic species (Llodrà-Llabrés et al., 2024).

In the lakes of the Sierra Nevada, the planktonic community coexists with three additional algal communities (Cuesta Linares et al., 2003; Sánchez Castillo and Morales Torres, 1980): (1) a bog-associated algal community comprising Chlorophyceae

(particularly Zygnemataceae and Desmidiaceae), along with diatoms and cyanobacteria, some of which are nitrogen-fixing (such as *Nostoc*, *Anabaena*, and *Cylindrospermum*); (2) epilithic biofilms primarily made up of cyanobacteria and diatoms and epipelic diatoms; and (3) algal mats predominantly composed of filamentous Zygnemataceae and cyanobacteria growing at the littoral and/or bottom of the lake.

2.3 Sediment coring and sampling

A slide-hammer gravity corer (Aquatic Research Instruments, Hope, ID, USA) with an inner core-tube diameter of 6.8 cm was used to collect a 26 cm sediment core (referred to as SSBG-21 hereafter) from the lake central area in September 2021. The sediment core was sectioned on-site following Glew et al. (2001) at 0.25 cm intervals for the first 9.25 cm and at 0.5 cm intervals for the remaining sediment with a core extruding apparatus provided by Aquatic research Instruments (http://www.aquaticresearch.com/core_extruding_apparatus.htm). For each section, 1 cm^3 were immediately taken from the centre of the core, using disposable material, and stored in small plastic polipropilene 5 cm^3 vials for pigment analysis avoiding the exposure of the sediment to light. The vials were completely full of sediment to avoid pigment degradation by oxygen and were kept at 4°C during transportation to the lab. Once in the laboratory, the vials were immediately placed at -80°C and at -20ºC after freeze-drying. The remaining sample was extruded into plastic zip-bags, later freeze-dried, and then stored at a desiccator.

2.4 Sediment chronology

Freeze-dried subsamples were analysed for ^{210}Pb, ^{226}Ra and ^{137}Cs by direct gamma spectroscopy in the Liverpool University Environmental Radioactivity Laboratory. A total of 18 subsamples between the top of the core and the 14 cm depth sediment were analysed. Sediment ages were estimated from unsupported ^{210}Pb activities using the constant rate of supply (CRS) and constant initial concentration (CIC) models (Appleby and Oldfield, 1978). ^{137}Cs was used as an additional dating marker, representing fallout emitted during thermonuclear bomb testing (with its peak in 1963) and nuclear accidents such as the Chernobyl accident in 1986.

2.5 Carotenoid pigment analysis

A total of 51 samples were used for pigment analyses, using freeze-dried sediments stored at -20 ºC in the dark. The pigments were extracted using 90% acetone with a probe sonicator (Sonopuls GM70 Delft, The Netherlands) (50 W, 2 min). The extract was centrifuged (4 min at 3000 rpm, 4°C), filtered through a Whatman ANODISC 25 (0.1 mm) filter and analyzed with ultrahigh-performance liquid chromatography (UHPLC) following a modification of the method described by Buchaca and Catalan (2007). The UHPLC system used was a Waters Acquity UPLC equipped with a PDA detector (λ 300–800 nm), refrigerated autosampler (4 °C), and upgraded with a Hexa/THF kit and 20 µL loop (Waters, Milford, MA, USA). Analytical separations were performed on an HSS C18 SB column (100 × 2.1 mm, 1.8 µm particle size) at 25 °C. The PDA channel was set at 440 nm for pigment detection and quantification. Peak integration was performed automatically using Empower software (Waters Corporation), which controls the UHPLC system. After sample injection (7.5 µL), a constant flow rate of 0.7 mL

175 min^{-1} was maintained. Pigments were eluted using a linear gradient from 100% solvent B (51:36:13
176 methanol:acetonitrile:Milli-Q water, v/v/v, with 0.3 M ammonium acetate) to 75% B and 25% A (70:30 ethyl
177 acetate:acetonitrile, v/v) over 3 min, followed by a 0.45 min isocratic hold at 75% B and a 2 min gradient to 100% A. Initial
178 conditions (100% B) were restored in 0.65 min, with a 1 min re-equilibration before the next injection. To address
179 reproducibility, chromatographic performance was evaluated by calculating the relative standard deviation (RSD) for retention
180 times and peak areas across replicate injections. All pigments exhibited RSD values within commonly accepted limits for
181 HPLC analyses (typically ≤1% for retention time and ≤2% for peak area), confirming that the method provides consistent and
182 reliable results under the tested conditions.

183 Pigments were identified by comparison with a library of pigment spectra obtained from extracts of pure algal cultures from
184 the Culture Collection of Algae and Protozoa (CCAP, Oban, Scotland, UK) and pigment standards (DHI Water and
185 Environment, Hørsholm, Denmark). β-carotene, a ubiquitous pigment present across algal groups, together with a suite of
186 carotenoids with high taxonomic affinity was selected for analysis. These marker pigments included scytonemin (UV-screen
187 pigment in cyanobacteria), alloxanthin (cryptophytes), aphanizophyll (N_2-fixing cyanobacteria), canthaxanthin and echinenone
188 (mainly cyanobacteria and zooplankton), astaxanthin (zooplankton and some chlorophytes), diadinoxanthin (mainly
189 dinoflagellates), diatoxanthin (diatoms), zeaxanthin (chlorophytes, zygnematophytes and cyanobacteria) and lutein
190 (chlorophytes and zygnematophytes). We based our interpretation on carotenoid profiles instead of phorbins because
191 carotenoids are less prone to degradation to colourless compounds (Buchaca and Catalan, 2008). Values for β-carotene were
192 expressed as nmol g^{-1} DW and used as a proxy for total algal community biomass, whereas concentrations of the ten selected
193 marker pigments were expressed as relative abundances (%) of their summed concentrations (excluding β-carotene). The
194 molecular weights of the different pigments were obtained from Jeffrey et al. (1997).

195 **2.6 Biological and paleo-environmental data analysis**

196 A total of 51 samples were used for C/N, $\delta^{15}N$ and for visible reflectance spectroscopy (VRS) inferred Chl-a and DOCw
197 analyses. The carbon to nitrogen (C/N) ratio is commonly used to identify organic matter sources in lacustrine sediments and
198 also potential N limitation on primary production. Algal-derived organic matter typically has C/N ratios between 4 and 10,
199 while terrestrial vascular plants show C/N ratios above 20. C/N values between 10 and 20 suggest a mix of both sources
200 (Meyers and Teranes, 2001). For elemental analyses of carbon and nitrogen content of the organic matter, a sediment fraction
201 of ~ 1 g of wet weight (WW) sediment was freeze-dried. To remove inorganic carbonates, samples were acidified in situ by
202 adding 1M HCl dropwise until effervescence ceased and overnight at 50 ºC. The elemental analysis was performed using a
203 Thermo Scientific Flash 2000 coupled to a mass spectrometer at the Scientific Instrumentation Center of the University of
204 Granada (CIC) determining the content of sediment C/N ratio calculated from the mass data and expressed as atomic ratios.

Nitrogen isotope ($\delta^{15}N$) composition was determined from the same bulk sediment organic matter used for the C/N analyses. It was performed on the remaining carbonate-free sediment samples using the elemental analyser Flash HT Plus coupled to IRMS DELTA V Advantage at the CIC.

Sediment samples were analysed for inferred trends in total lake-water organic carbon following the methodology described in Meyer-Jacob et al. (2017) and sedimentary chlorophyll-*a* including its derivatives (visible reflectance spectroscopy (VRS) inferred Chl-a) were analysed according to Michelutti et al. (2010) at the Paleoecological Environmental Assessment and Research Laboratory (PEARL), Queen's University (Canada). Briefly, prior to analyses, lyophilized sediment samples were sieved (125 µm mesh) to remove the influence of particle size and water content on the spectral signal. Next, VNIR spectra were recorded with a FOSS XDS Rapid Content Analyzer in diffuse reflectance mode. Each sediment sample spectra represents a mean of 32 scans at 2 nm resolution in the wavelength range from 400 to 2500 nm. For VRS-inferred chl-a, the absorbance peak of chlorophyll-a between 650 and 700 nm was considered in relation to calibration samples covering a range of sedimentary chlorophyll-a concentrations, as measured by high performance liquid chromatography (HPLC). Sedimentary VRS chl-a concentrations were inferred using log transformed data from Michelutti et al. (2010) with the equation: chl a + derivatives = EXP (0.83784 * LN (peak area 650–700 nm) + (−2.48861)). Our chlorophyll-*a* inferences, which include all algal and cyanobacterial groups, also include all chlorophyll isomers and its major derivatives (pheophytin and pheophorbide) (Michelutti et al., 2010; Michelutti and Smol, 2016). For inferred water TOC, an orthogonal partial least squares regression model between VNIR spectral information (400-2500 nm) and measured surface-water TOC concentrations in 345 lakes was used to reconstruct lake-water TOC levels from sediment samples (Meyer-Jacob et al, 2017). In our case, lake-water TOC is considered virtually equivalent to DOC in lake water due to the dominant contribution of DOC in the Sierra Nevada lake's organic carbon pool (Mladenov et al., 2008), a pattern also observed in lakes with similar characteristics (Meyer-Jacob et al., 2019). From this point onward, analyzed TOC in water will be referred to as DOCw, as we consider relative changes in TOC to reflect relative changes in DOC in the water.

2.7 Climate and atmospheric data input

The climate data that was used for statistical analysis to explore relationships with the pigment matrix was obtained from Sigro et al. (2024), who developed a high quality daily climate data base specifically for the Sierra Nevada Mountains (http://www.c3.urv.cat/climadata.php). We used the mean annual temperature anomaly (MATA) and annual precipitation anomaly (APA). Seasonal mean temperature anomaly (MTA)- springMTA, summerMTA, fallMTA, and winterMTA-, and seasonal precipitation anomaly (PA)- springPA, summerPA, fallPA, and winterPA-, were used to correlate with the annual climate data through Pearson's correlation analysis. Data were tested for normality before the analysis. This database has been quality-controlled and homogenized using CLIMATOL (https://climatol.eu/). Climate data was available for the period ~1894-2020 yr CE.

The intensity of Saharan dust emission and transport has been linked to the Sahel drought (Chiapello et al., 2005; Moulin and Chiapello, 2004). Furthermore, Jiménez et al. (2018) demonstrated that the Sahel Precipitation Index (SPI) can be utilised as a predictor of the transport and intensity of Saharan dust events in Sierra Nevada, reflecting atmospheric P and Ca deposition trends in this region. These indices exhibited strong correlations with the zirconium-to-aluminium (Zr/Al) ratio—a proxy for Saharan dust deposition—measured in a sediment core from one of the Sierra Nevada lakes, as well as with Saharan calcium concentrations in an ice core from the French Alps, which are indicative of Saharan dust events (Preunkert and Legrand, 2013). Consequently, SPI was employed for this purpose in the present study. The Sahel precipitation index (SPI), extending back to 1900 yr CE, was accessed from the NOAA Physical Sciences laboratory (https://psl.noaa.gov/data/timeseries/month/SAHELRAIN/). It provides a standardized rainfall index data for the Sahelian zone of northern Africa. Negative SPI values indicate severe drought conditions, significantly enhancing dust emission and atmospheric loading.

The annually resolved climate and dust metrics were averaged over the period of accumulation for each dated interval, i.e. the data were binned in exactly the same intervals as those obtained from the sediment core, thereby integrating the instrumental data with the paleolimnological data. Final weighted data are only available for the period 1905-2020 yr CE (corresponding to samples 1-22).

2.8 Statistical analysis

Before statistical analyses were applied, data were transformed to reduce the asymmetry of the distributions and to standardise them, i.e. remove incomparabilities in the total variance. The pigment variables (expressed as relative abundance) were square root transformed (Hellinger transformation) to minimize the impact of dominant species and handle the sparse nature of the dataset (presence of many zeros). The β-carotene pigment was excluded from the pigment matrix because it was considered to be a proxy for total algal biomass (Buchaca et al., 2019; Zhang et al., 2019). The explanatory biological and paleo-environmental variables ((C/N ratio, DOCw, chlorophyll-*a* and β-carotene) were logarithmically transformed followed by a relative scale transformation ($y' = y_i / y_{max}$) to remove asymmetry and incomparabilities in the total variance. The $\delta^{15}N$ values were used untransformed as these met the conditions of normality and homoscedasticity. Finally, the climate and dust metric variables (MATA, APA, and SPI) were relative scale transformed. All transformed variables met the assumptions of normality and homoscedasticity for the application of parametric statistics

The number of significant pigment zones (CONISS; constrained hierarchical clustering; Grimm, 2011) was determined using the broken stick model (Bennet, 1996). Principal component analysis (PCA) was performed on the matrix of individual pigments to summarize the major patterns of variability in pigment assemblages into a few axes. Previously, detrended correspondence analysis (DCA) results (gradient length <2 SD) indicated that linear ordination was most appropriate (Legendre and Birks, 2012).

Redundancy analysis (RDA) was conducted to identify the climate and atmospheric explanatory variables of algal assemblage changes. Generalized linear models (GLM) analysis was conducted to explore climate and atmospheric drivers of the main variables reflecting primary producer abundance (VRS-inferred Chl-*a* and β-carotene). Both analyses were performed for the period during which atmospheric and climate data were available (~1905-2020 yr CE; 22 samples). The explanatory variables used in both analyses included annual temperature (MATA), precipitation data (APA) and SPI. Seasonal temperature and precipitation data were not included in these analyses to reduce the number of explanatory variables. Pearson correlations between annual and seasonal climate variables were performed.

The RDA (with forward/backward selection) was performed to identify the statistical independence and relative strength of each of the explanatory variables (MATA, APA and SPI) of the pigment assemblage changes, using Monte Carlo permutation tests (999 unrestricted permutations) with a significance level of $p < .05$. Akaike's information criterion (AIC) (Burnham and Anderson, 2004) was used to extract the environmental variables that significantly increased the amount of explained variation of pigment data, thereby optimising the global AIC. AIC was selected because it helps identify the most parsimonious model for explaining the variation in algal community assemblage. Significant environmental variables were incorporated into the final model and subjected to RDA once again.

In the GLM analyses, the optimum model was selected using Akaike's information criterion adjusted for sample size (AICc; Burnham and Anderson, 2004). Models with an AICc difference of less than 2 compared to the lowest AICc were considered the best models and statistically equivalent. The contribution of each variable to the final model was determined by assessing its significance and percentage of variance explained. Residuals of the final models were examined to check for normality of data and absence of over-dispersion.

Ordination and model selection analyses were performed using the vegan (Oksanen, J., 2022) and the MuMIn (Multi-Model Inference; Bartón, 2025) packages for the R software environment, respectively. In all the analyses the variance inflation factor (VIF) was used to eliminate highly correlated variables before applying analyses. All the explanatory variables that yielded VIFs >5 were eliminated in the analysis due to the high degree of collinearity.

3. Results

3.1 Geochronology

The Borreguil lake record consists of 26 cm of peaty (primarily bryophytes) and silty clays. The total activity of ^{210}Pb (Fig. 2A) reached levels close to equilibrium with the supporting ^{226}Ra at a depth of 6-7 cm in the core SSBG-21. According to the CRS and CIC models (Appleby and Oldfield, 1978), the concentrations of unsupported ^{210}Pb below 1 cm decrease exponentially with depth (unshown data). This indicates a relatively uniform accumulation of sediments over much of the time period spanned by the core. The relatively uniform concentrations observed in the top 1 cm may be attributed to a recent slight

increase in sedimentation rates. Excluding the top 1 cm, the average sedimentation rate is calculated to be 0.0098 ± 0.008 g cm^{-2} y^{-1} (or 0.041 cm y^{-1}) (Fig. 2B). Additionally, ^{137}Cs concentrations showed a distinct peak at a depth of 1.5-1.75 cm (Fig. 2A), likely reflecting fallout from the Chernobyl accident in 1986. The reliable dating period for the core extends from 6.63 cm to the present, covering approximately ~1850 to 2020 yr CE, with an estimated mean temporal resolution of 5 years per sampling interval. The ^{210}Pb chronology only constrains the upper part of the sediment sequence, whereas ages assigned to deeper intervals rely on extrapolation of sedimentation rates beyond the dated section. This approach implicitly assumes constant sedimentation through time, negligible compaction, and the absence of hiatuses or sediment mixing, assumptions that we acknowledge explicitly given the lack of independent chronological control below the ^{210}Pb-supported interval. Therefore, the inferred basal age (~400 years) and the temporal interpretation of deeper sediments should be taken cautiously.

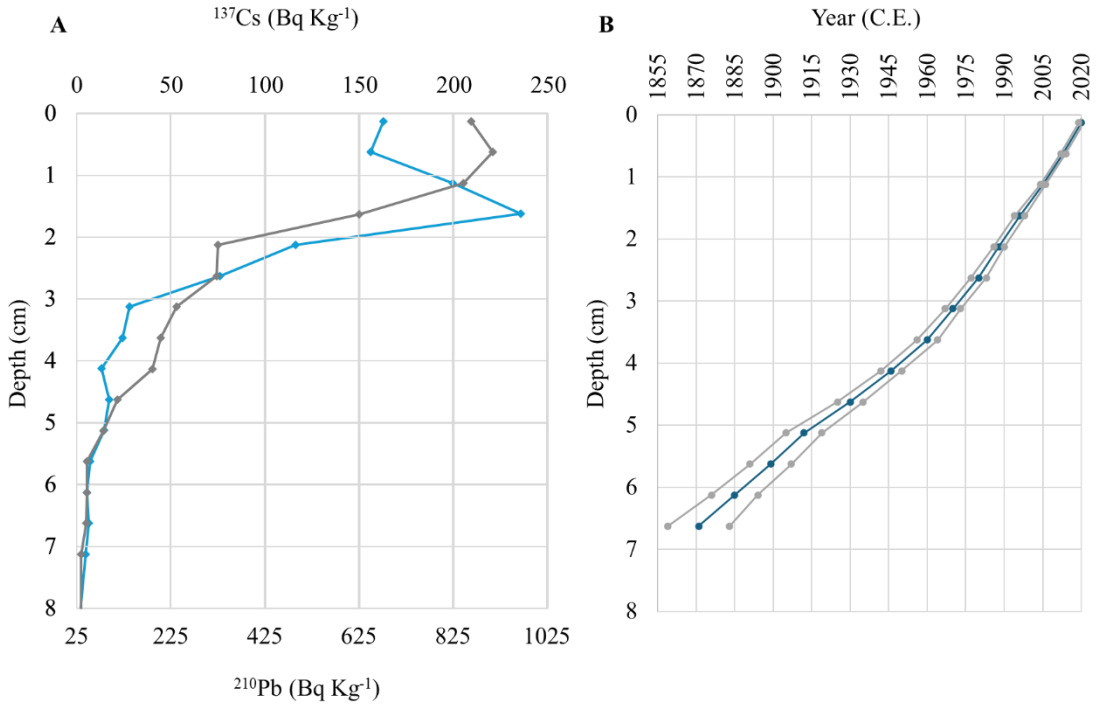

Figure 2: A) Radiometric chronology showing ^{210}Pb (grey line) and ^{137}Cs (blue line) activity (bq kg^{-1} dried sediment) from sediment core SSBG-21 extracted from Borreguil Lake. B) ^{210}Pb-estimated age (using the constant rate of supply model) versus core depth (black line) and the associated errors (grey lines).

3.2 Trends in pigment composition and other paleoenvironmental variables

Throughout the whole core, the pigments associated with Chlorophyceae and Zygnematophyceae (lutein and zeaxanthin) and those associated with diatoms (diatoxanthin) were predominant (Fig. 3, Fig. S2). Both lutein and zeaxanthin were attributed to an origin in green algae, given that their concentration profiles change in parallel (Fig. S2). Other significant pigments are

317 those associated with cyanobacteria (aphanizophyll, echinenone and scytonemin) (Table S2). The least abundant pigments
318 were diadinoxanthin (a marker pigment for Dinophyceae) and alloxanthin (a marker pigment of cryptophytes), which remained
319 below5% abundance throughout the profile (Fig. 3). In addition to the aforementioned pigments, astaxanthin and
320 canthaxanthin, typically associated with zooplankton, were also detected (Fig. 3, Table S2). Supplementary Figure S2 and
321 table S2 show the pigment profiles expressed as concentrations (nmol PGM / g DW) and all the pigments identified together
322 with their taxonomic affinities, respectively. In shallow high-mountain lakes, pigment records are often affected by intense
323 photo-oxidative processes in the water column. To evaluate whether such processes influence downcore variability, we
324 assessed pigment preservation using the Chl-a/a-phorbins index (Fig. S2), which remains remarkably constant throughout the
325 sediment sequence. This indicates that, while overall pigment degradation may be high, preservation conditions have not
326 changed substantially through time, and therefore relative stratigraphic trends are unlikely to result from variable degradation.
327 In these systems, sedimentary pigment assemblages reflect an inherent integration of primary producers from both the water
328 column and benthic biofilms developing at or near the sediment surface. Previous studies in Pyrenean lakes have demonstrated
329 that lake depth largely controls the relative importance of planktonic versus benthic pigment signals, with shallow lakes
330 showing a stronger benthic imprint and short transport distances between production and deposition (Buchaca and Catalan,
331 2007, 2008). Thus, pigment-based reconstructions in Borreguil Lake should be interpreted as recording relative changes in
332 integrated photoautotrophic communities.

333 Results are described using a stratigraphically constrained cluster analysis based on pigment composition (excluding chl-*a* and
334 β-carotene) (Fig.3). According to the CONISS analysis the sediment pigment sequence can be divided in five significant zones
335 of change (Fig. 3) with changes at ~1970, ~1843, ~1804, and ~1690 yr CE.

336 Zone 1 (between 1600 and 1690): This period is characterised by the highest levels of lutein, as well as relatively
337 high levels of diatoxanthin and zeaxanthin. This indicates a period of dominance by diatoms and green algae. Other pigments
338 present in this zone are astaxanthin and canthaxanthin, which show particularly highly abundances during this interval. In
339 contrast, VRS-inferred Chl-*a* and β-carotene, both indicators of overall algal biomass, show the lowest values recorded in the
340 entire sequence.

341 Zone 2 (between 1690 and 1804): A decrease in lutein accompanied by an increase in diatoxanthin indicates a shift
342 toward greater dominance of diatoms over green algae. The diversification of the algal community is notable during this period.
343 Pigments associated with cyanobacteria, such as echinenone and aphanizophyll, appeared for the first time, although they were
344 present in low concentrations. Notably, echinenone production began to increase around 1750 CE and remained relatively
345 stable at around 5% until the top of the core, whereas aphanizophyll showed low abundances between 1750 and 1800 CE
346 before disappearing. Scytonemin, a pigment associated with the UV protection in cyanobacteria, also appeared at this time,
347 albeit at very low relative abundances. Diadinoxanthin, a marker pigment for Dinophyceae, was first recorded around 1750
348 CE. Astaxanthin and canthaxanthin exhibited their highest values during this period. These pigments were most abundant from
349 the bottom of the core to around 1750 CE, after which there was a progressive decline to the top of the core. Indicators of algal

biomass (VRS-inferred Chl-*a* and β-carotene) and the C/N ratio show the lowest values on record during the first half of the period (until around 1750 CE), but increase during the second half, exhibiting significant fluctuations with several peaks and troughs.

Zone 3 (between 1804 and 1843): In the algal assemblage, an increase in green algae (indicated by lutein) is observed at the expense of diatoms (represented by diatoxanthin). All pigments detected in the previous period remain in this one, with the exception of aphanizophyll, which disappears. This interval is also characterised by high peaks in VRS-inferred Chl-*a*, β-carotene, C/N ratios and DOCw.

Zone 4 (between 1843 and 1970): There are few changes observed in the algal assemblage, which largely appears to be a continuation of the previous period, except for the reappearance of aphanizophyll. The concentration of diadinoxanthin (a marker pigment for Dinophyceae) declined from 1870 CE onwards, while alloxanthin first appeared around 1900 CE, maintaining low concentrations until the top of the core. In contrast, more pronounced changes are evident in other paleoenvironmental variables (Fig. 3). C/N and DOCw show fluctuating values, whereas $\partial^{15}N$ decreases slightly during this period. VRS-inferred Chl-*a* and β-carotene show low values until approximately 1900 CE, after which they show a marked increase.

Zone 5 (between 1970 and 2020): This period exhibits the most pronounced changes in the entire record. The highest values recorded for VRS-inferred Chl-*a* and β-carotene are observed during this interval. The abundance of diatoxanthin declined from 1970 towards the top of the core, whereas the abundance of lutein and zeaxanthin increased. This indicates a shift in dominance from diatoms to green algae. These post-1970 changes coincide with a significant increase in temperature (MATA) and Saharan dust deposition (SPI) in the Sierra Nevada (Fig. 4).

Echinenone production maintains a stable abundance of around 5% throughout the core (Fig. 3). This suggests that either the primary producer (cyanobacteria) or the transformation pathway (the degradation of other pigments into echinenone) is constantly operating, regardless of climate and environmental factors. Aphanizophyll, which is produced by nitrogen-fixing cyanobacteria, shows the highest values (10%) towards the top of the core (Fig. 3). This increase coincides with a steep decline in $\delta^{15}N$ values, suggesting NOx transformation and fixation by N2-fixing cyanobacteria. Aphanizophyll exhibits a strong negative Pearson correlation with $\delta^{15}N$ ($r = -0.84$), and the two variables display opposite profiles throughout the entire core (Fig. 3). A steep decline in C/N ratio values are also recorded at this period. Scytonemin, a pigment associated to protection against UV light, persisted at 2% until the top (Fig. 3). DOCw values, a good estimator of UV transparency (Laurion et al., 2000), show an increase since ~1975. The least abundant pigments were diadinoxanthin (a marker pigment for dinoflagellates) and alloxanthin (a marker pigment for cryptophytes), with an abundance of less than 5% throughout the record (Fig. 3).

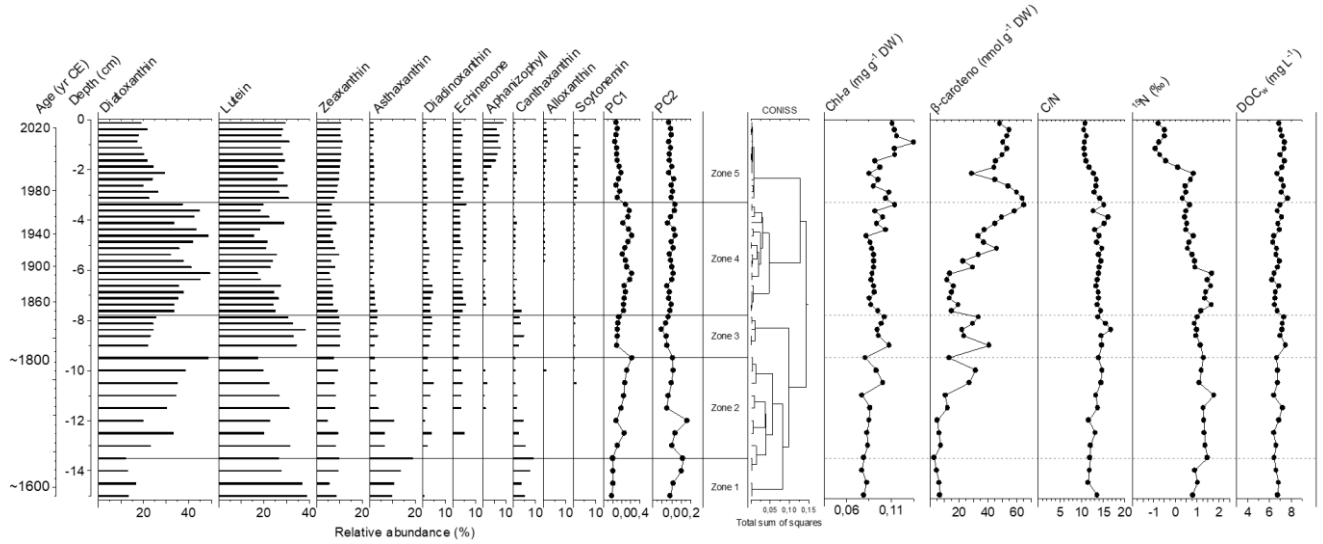

Figure 3: Relative abundance diagrams of the sedimentary pigments and evolution of selected paleoenvironmental variables recorded in the sediment core SSBG-21 in Borreguil Lake. The axis 1 and 2 of the PCA performed on pigment data and the result of a cluster analysis of pigment assemblage data using constrained incremental sum of squares (CONISS) are shown. The black lines represent the main zonation identified by the broken stick model. The data are plotted against the sediment depth (cm, primary y-axis) and on age (yr CE, secondary y-axis). Dates prior to 1850 should be interpreted with caution, as the age provided is beyond the confidence dating provided by stable radioisotopes.

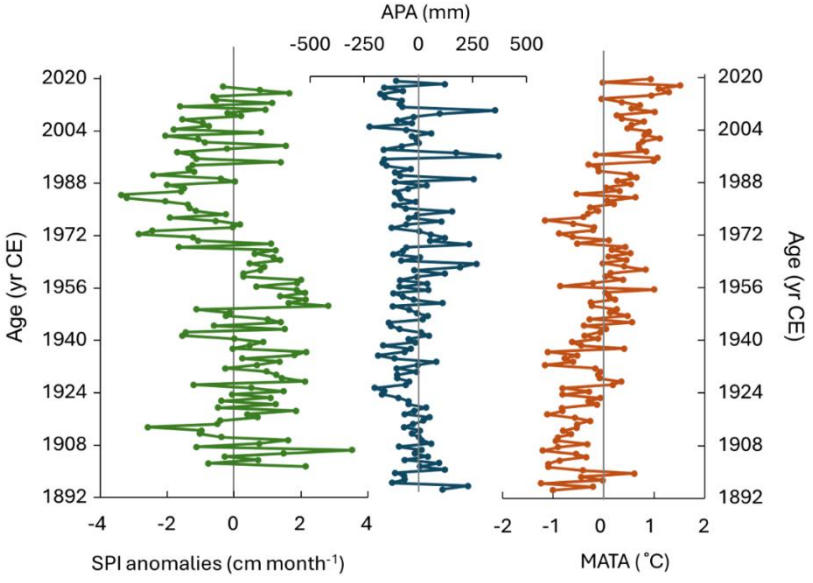

Figure 4: Evolution of the climatic variables MATA (mean annual temperature anomalies for air), and APA (annual precipitation anomalies) at the summits of Sierra Nevada for the period 1894-2020, and Saharan dust metric SPI (Sahel Precipitation Index). All are instrumental data. Temperature and precipitation data were obtained from Sigró et al. (2024). The anomalies of the SPI are calculated with respect to 1900 and 2013 and based on June through October averages for each year.

Regarding climate variables, Mean Annual Temperature Anomalies (MATA) increased steadily from 1905 to 1970, while Annual Precipitation Anomalies (APA) decreased slightly until 1920 and then increased slightly (Fig. 4). The Sahel Precipitation Index (SPI) shows relatively high values (less dust in the atmosphere) with no significant changes. The SPI record (Becker at al., 2013) indicated a predominantly wet period (positive values) in the Sahel from 1900 yr CE to approximately 1970 yr CE (Fig. 4).

A significant increase in temperature (MATA) and Saharan dust deposition (SPI) in the Sierra Nevada (Fig. 4) was observed post-1970. The warming in MATA was mainly driven by summer and spring temperatures (Sigro et al., 2024). This trend was also observed in the correlation analysis, which yielded a correlation factor of 0.97 and 0.94 between MATA, and summer and spring mean temperatures, respectively (Supplementary Fig. S3). Mean annual (Fig. 4) and seasonal mean temperatures (Supplementary Fig. S4) show negative anomalies prior to the 1940s and there were negative values around the 1970s. Regarding the precipitation anomalies, a downward trend was observed during the period 1975–2020 yr CE, which exhibited a significant negative trend of -12.9% per decade in summer precipitation (Fig. 4; Sigró et al., 2024). The SPI record indicated a relatively stable and dry period (negative values) from around 1970 yr CE to the present, with the lowest values observed during the 1980s-1990s yr CE (Fig. 4). Substantial negative SPI values indicate severe drought conditions, significantly enhancing dust emission and atmospheric loading (Jiménez et al., 2018).

3.3 PCA of the pigment matrix

PCA of the 51 core samples explained 73.91% of the total pigment variation (45.84% for axis 1 and 28.07% for axis 2) (Fig. 5). Axis 1 showed two periods: a decrease until ~1670 yr CE and an upward trend after that, with some fluctuations (Fig. 3). Axis 2 tracked an increasing trend around ~1705-~1780 yr CE and ~1850-~1900 yr CE, followed by a sharp decline after ~1970 yr CE (Fig.3). Axis 1 was linked to echinenone, aphanizophyll, diadinoxanthin, and alloxanthin in the positive region, and Crustacea-related pigments (astaxanthin, canthaxanthin) in the negative region (Fig.5). Axis 2 was associated with zeaxanthin, lutein, and diatoxanthin, with scytonemin showing no clear relationship to either axis.

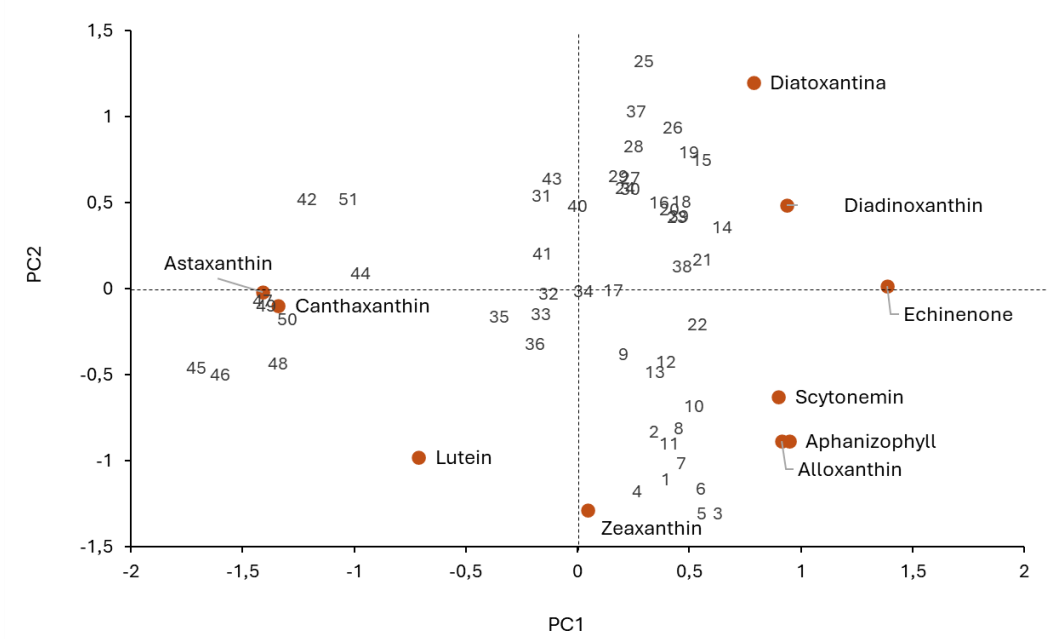

Figure 5: Principal component analysis (PCA) biplots of the pigment assemblages from sediment core SSBG-21 extracted from Borreguil Lake for the last ~430 years. Numbers refer to the sample sites being 1 the most modern sample and 51 the oldest sample.

3.4 Relationships between pigment data and instrumental climate data over the last 115 years

Prior to all the analyses, VIF>5 analyses were performed on the explanatory variables and no variables were discarded. The resulting RDA model produced an R^2 adjusted value of 0.468, with MATA and SPI identified as the primary drivers of pigment composition across the period ~1905-2020 yr CE (Fig. 10; Table 1).

To explore the relationships between VRS-inferred Chl-*a* and β-carotene and annual climate and atmospheric variables, GLM analyses were undertaken (Table 2). MATA was selected as the main explanatory variable for VRS-inferred Chl-*a* and β-carotene, being APA secondary explanatory variable for β-carotene.

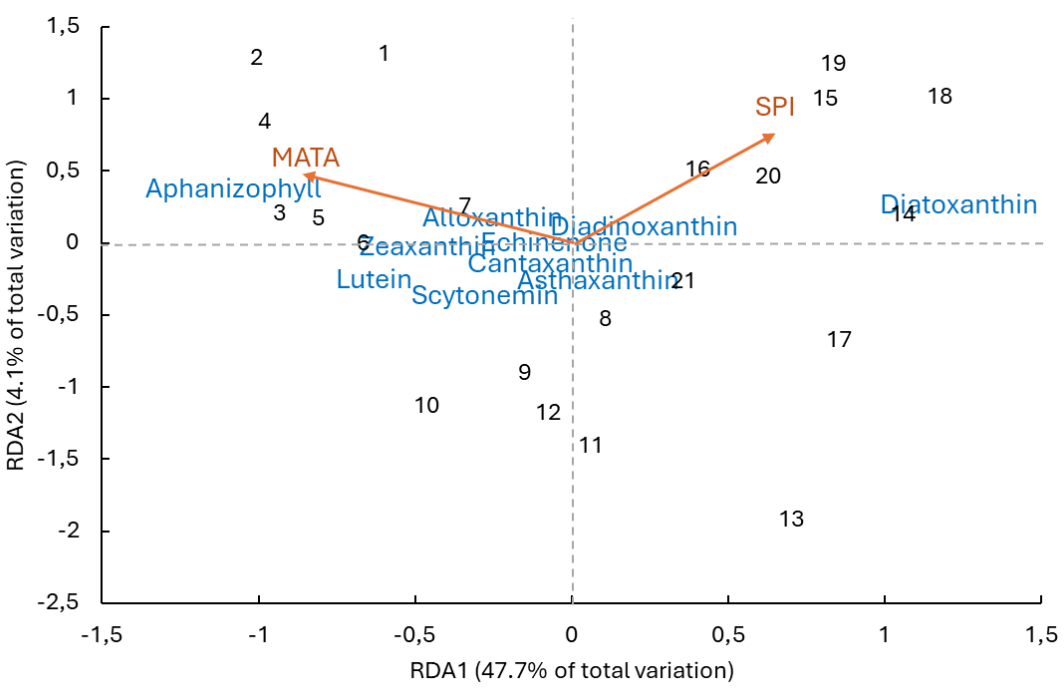

Figure 6: The results of the Redundancy Analysis (RDA) ordination plot showing the relationship between pigment assemblages data from sediment core SSBG-21 and the climate and atmospheric variables. The selected explanatory variables by the RDA analysis are shown: MATA (Mean annual air temperature anomalies) and SPI (Sahel Precipitation Index as proxy of Saharan dust input). Only the first two RDA axes are shown. Sample sites (representing sediment intervals) are also shown, being "1" the most modern interval and "22" the oldest one. See Table 1 for more details of the analysis results.

Table 1: Summary of results from the redundancy analyses (RDA) with pigment matrix as response variable and the climate variables as explanatory variables for BG Lake for the period ~1905-2020. Forward/backward-selection was used to select the explanatory variables for the RDA, that were scale-relative transformed to standardize to mean variance. Only selected predictor variables for the RDA are shown. Adj R^2 = Adjusted R^2. Significance levels: *** P < 0.001; ** 0.001 < P < 0.01.

	df	Variance	F	p-values
MATA	1	0.787	11.626	0.001***
SPI	1	0.412	6.091	0.004**
Residual	19	1.29		
Adj R^2	0.468			

Table 2: Summary of results from the model selection analyses (generalized linear models-GLM) predicting the VRS-inferred Chl-*a* and β-carotene for BG Lake for the period ~1905-2020. The explanatory variables were relative scale transformed to standardize to mean variance. The best model according to the Akaike's information criterion (AICc) values is shown. Predictor variables for the analyses include: MATA, Sierra Nevada mean annual air temperature anomaly; APA, Sierra Nevada annual precipitation

anomaly and SPI, Sahel precipitation index (proxy for Saharan dust input). Adj R^2, adjusted R^2. * Significance level $p < 0.001$; * Significance level $0.01 < p < 0.05$.**

Response variable	Explanatory variables	Adj R^2	χ^2 = LRChisq	df	p-values
VRS-inferred Chl-*a*	MATA	0.419	16.125		$5.93 \cdot 10^{-5}$ ***
β-carotene	MATA	0.185	3.920	1	$4.77 \cdot 10^{-2}$ *
	APA		3.355	1	$6.70 \cdot 10^{-2}$ *

4. Discussion

In this study, we have employed different proxies (algal subfossil pigment assemblages and other paleoenvironmental biological variables) derived from the Borreguil Lake sediment core with the objective of gaining a deeper understanding of past regional climate-driven changes for Sierra Nevada lakes and alpine lakes in general. The algal community exhibited notable changes, both in the algal biomass and assemblage composition throughout the entire core (1600 yr CE-present), which were mainly driven by climate and atmospheric variables. The most pronounced changes, both in algal biomass and assemblages, occurred during the latter half of the twentieth century coinciding with a period of marked rise in temperature and Saharan dust deposition driver, and a decreasing trend in the precipitation.

4.1 Changes in the algal biomass

The long-term changes in primary production and/or algal biomass throughout the core was assessed by the combined analysis of VRS-inferred Chl-*a* and β-carotene, indicators of algal biomass. Both variables show similar trends throughout the core. From the bottom of the core to around 1750 yr CE, both remained stable and low, reaching their lowest levels. This low biomass period may be linked to low temperatures during the Little Ice Age (LIA), as shown by Jiménez-Moreno et al. (2023) for Río Seco Lake in Sierra Nevada and from Oliva et al (2018) for the Iberian Mountains. Between ~1750 and 1800 CE, concentrations of VRS-inferred Chl-*a* and β-carotene fluctuated, reaching peak levels, despite this period coinciding with the lowest temperatures of the Little Ice Age (LIA) in the Sierra Nevada, according to Jiménez-Moreno et al. (2023). Although we do not have a clear explanation for this increase, we hypothesize that this phenomenon may be attributed to reduced herbivory pressure (reduction of astaxanthin and canthaxanthin), as the development of herbivore populations is constrained by the brief duration of ice-free periods. However, Oliva et al. (2018) indicate that the period 1760–1800 CE was a time of climate extremes in the Iberian Mountains, which could explain the fluctuations observed in Chl-*a* and β-carotene in the Sierra Nevada during that period.

At the end of the LIA (1800-1840 yr CE), a temperature peak at the Sierra Nevada summit was recorded (García-Alix et al., 2020; Jiménez-Moreno et al., 2023). The observed algal biomass increase at the 8–10 cm depth of our record was likely related to this temperature peak (although the uncertainty of our dating prior to 1850 should be noted) and is consistent with trends in

other mountain lakes (Hu et al., 2014; Huo et al., 2022; Lami et al., 2010; Oleksy et al., 2020). Moreover, the C/N peak ~1840 yr CE suggests an influx of external organic matter, potentially driven by thaw-induced transport. The main changes in VRS-inferred Chl-*a* and β-carotene occurred from ~1920 yr CE onwards, when a striking increase in both variables was observed. This biomass increase has no precedent in the last 400 years in the lake and according to GLM analysis (Table 2), climate factors—particularly rising temperatures—were identified as the main drivers of these changes. In alpine lakes, higher temperatures and lower precipitation may extend the ice-free period (Anderson et al., 1996; Rogora et al., 2018), increasing the growing season and resulting in a higher accumulation of annual algal biomass. Moreover, longer ice-free seasons in alpine lakes boost light availability, water temperature, and solute inputs through snowmelt and weathering (Preston et al., 2016; Sommaruga-Wögrath et al., 1997) all enhancing biological production (Douglas and Smol, 2010; López-Merino et al., 2011). These facts were observed across the Sierra Nevada lakes (Jiménez et al., 2018) and across arctic and alpine lakes (Adrian et al., 2009; Rühland et al., 2008, 2015). We therefore suggest that temperature controls how much biomass is produced in the lake. This means that the big rise in temperature and fall in rain in summer in Sierra Nevada (Supplementary Fig. S4; Sigro et al., 2024) could be the reason for the large and unprecedented increase in the amount of algae since the 1960s yr CE to the present.

Additionally, Saharan dust may increase nutrients in Borreguil Lake, boosting algal production. Sierra Nevada has experienced an increase in the frequency of dust events particularly since the 1970s yr CE. Longer ice-free periods may have further amplified dust exposure, boosting nutrient availability and promoting algal growth (Korbee et al., 2012; Saros et al., 2005; Yang et al., 1996). Saharan dust inputs influence the structure and composition of biological communities in Sierra Nevada lakes. For example, phosphorus inputs enhance algal biomass, leading to higher chlorophyll-*a* concentrations (Carrillo et al., 1990; Morales-Baquero et al., 2006). Similar Saharan dust fertilization effects have been observed in the Pyrenees (Camarero and Catalán, 2012). Recent results from Borreguil Lake show that, in 2022 yr CE, following a massive influx of Saharan dust in Sierra Nevada, there was a significant increase in phytoplankton water column density and a shift in the lake algal composition, with a marked increase in the percentage of cyanobacteria (Supplementary Fig. S1). Thus, the increase in algal biomass in Borreguil Lake since the 1970s can be attributed primarily to temperature and secondarily to Saharan P input.

Since the early 1900s yr CE, anthropogenic nitrogen deposition has become increasingly evident in lake sediment cores from high-latitude regions of the American Northern Hemisphere (Holtgrieve et al., 2011), particularly during the latter half of the 20th century (around the 1970s), coinciding with the "Great Acceleration" of global environmental change (Steffen et al., 2007). It is conceivable that nitrogen deposition has influenced the increase in algal biomass observed in Borreguil Lake and the sharp decline in the C/N ratio post-1970 CE could reflect this N enrichment in the lake. However, nitrogen deposition in Sierra Nevada is lower than in other Mediterranean regions (Morales-Baquero et al., 2006, 2013) and heavily industrialized areas of Central Europe (Holland et al., 2005), with a mean total nitrogen deposition (dry and wet) of 115.2 mg m^{-2} d^{-1} between 2000-2002 yr CE. Moreover, the parallel dynamics between the C/N ratio and the $\delta^{15}N$ ratio, as well as the increase in

Aphanizophyll, suggest that N enrichment in the lake is associated with an increase in N_2-fixing cyanobacteria. Therefore, it is unlikely that the increase in algal biomass in Borreguil Lake was mainly influenced by atmospheric N deposition.

4.2 Changes in the composition of the algal community

4.2.1 Period ~1600-1804 yr CE

From the core bottom to ~1750 yr CE, pigments from chlorophytes, diatoms, and Crustacea (canthaxanthin, astaxanthin) dominated. After ~1750 yr CE, crustacean pigments declined, remaining below 5% thereafter. The decline in crustacean abundance could have coincided with the LIA minimum temperatures in the Sierra Nevada (1750–1800 yr CE) according to Jiménez-Moreno et al., 2023) during which colder conditions may have hindered zooplankton communities (Morales-Baquero et al., 2006). However, Oliva et al (2018) indicate a period of climatic fluctuations from 1750-1800 and this is consistent with the diversification of the algal community (appearance of diverse pigments) from 1750 onwards in Borreguil Lake. The fluctuations in algal biomass further suggest a period of climatic variability.

4.2.2 Period ~1804-1970 yr CE

The main change in pigment composition took place at ~1840 yr CE, as indicated by the CONISS analysis and the PCA axis 1 (Figs. 3 and 5). This change in pigment composition was characterized by the first appearance of aphanizophyll and a decrease in canthaxanthin and astaxanthin. This change may be explained by a summer temperature peak in Sierra Nevada (based on chironomids and leaf waxes) between 1800 and 1840 yr CE (García-Alix et al., 2020; Jiménez-Moreno et al., 2023) at the end of the LIA. Warming could explain the increased relative abundance of cyanobacteria, which take advantage at higher temperatures (Havens and Paerl, 2015). This change in pigments around 1840 CE corresponds with global shifts in aquatic ecosystems since the mid-19th century, which have been caused by human activity (Dubois et al., 2018). However, the Sierra Nevada was not directly affected by humans during this period (Anderson et al., 2011; García-Alix et al., 2013). Therefore, the observed change is probably due to climate warming at the end of the LIA.

The period from 1840 to 1970 yr CE was characterized by the absence of significant shifts, with the algal community remaining essentially unchanged. This stability between 1840 and 1970 may be explained by the relatively moderate temperature increase during that period of approximately 1 ºC according to Jiménez-Moreno et al., (2023) and Oliva et al. (2018).

4.2.3 Period ~1970-2020 yr CE

From ~1970 yr CE onwards, significant shifts in pigment assemblages were observed, characterized by increases in cyanobacteria (aphanizophyll, scytonemin), cryptophytes (alloxanthin), and green algae (lutein, zeaxanthin), while diatoms (diatoxanthin) decreased.

4.2.3.1 Increase in the relative abundance of cryptophytes, cyanobacteria and chlorophytes

Our RDA results reveal that mean annual temperature and Saharan dust deposition were key drivers of pigment assemblage changes, with temperature being the primary factor. The temperature increase since the 1970s yr CE likely favoured taxa with higher thermal optima, such as green algae (Barone and Naselli-Flores, 2003; Elmslie et al., 2020; Florian et al., 2015) and cyanobacteria (Havens and Paerl, 2015), over diatoms. Additionally, phosphorus enrichment in the lake during this period may have enhanced the performance of chlorophytes, cyanobacteria, and cryptophytes (Buchaca and Catalan, 2024; Zufiaurre et al., 2021) in Borreguil Lake. For example, Oleksy et al. (2020) demonstrated that, in high mountain lakes, the rise in chlorophytes and cyanobacteria was mainly driven by climate warming and phosphorus. In addition, the input of Ca-rich Saharan dust may have promoted cyanobacterial growth over diatoms. This is supported by the results of several authors (Brahney et al., 2015; González-Olalla and Brahney, 2025) who suggest carbonate-rich dust enrichment led to greater cyanobacteria growth in an alpine lake. In Borreguil Lake the large influx of Saharan dust in 2022, for instance, led to a marked increase in the proportion of planktonic cyanobacteria (Supplementary Fig. S1).

4.2.3.2 Increase in the relative abundance of N_2-fixing cyanobacteria

Saharan phosphorus input into the lake may have caused a stoichiometric imbalance, leading to N-limitation of the primary production that favoured potentially N_2-fixing cyanobacteria (aphanizophyll). If N is limited, N_2-fixing cyanobacteria (aphanizophyll) may still result in high productivity and lower the $\delta^{15}N$ data as the isotopic signature of N_2 is also low. The decline of the C/N ratio after 1970 could be partly the result of an enrichment of organic matter in nitrogen due to nitrogen fixation. Significant decline in $\delta^{15}N$ values have been observed in high-altitude lakes across America (Holtgrieve et al., 2011; Spaulding et al., 2015; Wolfe et al., 2003), the Alps (Hofmann et al., 2021), and Arctic regions (Florian et al., 2015) primarily attributed to increased atmospheric nitrogen deposition. However, the sharp decrease in $\delta^{15}N$ values at ~1990 yr CE in our study contrasts with the observed decline in nitrogen deposition in Europe after 1980 (Engardt et al., 2017). Moreover, in the Sierra Nevada region, nitrogen deposition is relatively low. On the other hand, the depletion of $\delta^{15}N$ due to N_2 fixation by cyanobacteria, driven by low nitrogen availability in Borreguil Lake, is supported by several factors. First, since the 1980s yr CE, the deposition of P-rich Saharan dust has increased in Sierra Nevada lakes (Fig. 6). In this regard, Camarero and Catalan (2012) report that increased Saharan atmospheric phosphorus deposition in recent decades has shifted lake phytoplankton from phosphorus limitation to nitrogen limitation in the alpine lakes of the Pyrenees. Second, Sierra Nevada experienced recurrent summer droughts since the 1980s yr CE (Pardo-Igúzquiza et al., 2024) resulting in a marked decline in wet deposition, which is the primary pathway for atmospheric nitrogen input into the lakes (Castellano-Hinojosa et al., 2017; Morales-Baquero et al., 2013). Additionally, lower precipitation reduces nitrogen transport from the catchment to lakes, further decreasing nitrogen input (Morales-Baquero et al., 1999). The high phosphorus Saharan dust deposition over the past 50 years, especially during the ice-free period, it likely has a greater impact on lake biota compared to nitrogen deposition, which is more concentrated during the ice-cover period. Together, these factors may have led to a reduction in nitrogen availability and favoured the growth

of N_2-fixing cyanobacteria, causing a decline in $\delta^{15}N$ values linked to N_2 fixation (Meyers and Teranes, 2001) and a decline also in C/N ratio.

Selective nitrogen loss during early diagenesis may contribute to part of the observed variability in C/N ratios and $\delta^{15}N$ values. However, the relatively low and stable C/N ratios (~8–15), the absence of a strong inverse C/N–$\delta^{15}N$ relationship, and the coherent increase in productivity proxies argue against diagenesis as the dominant control. Importantly, the co-occurrence of low $\delta^{15}N$ values with the presence of aphanizophyll provides independent evidence for an enhanced contribution of newly fixed nitrogen during this interval, with diagenetic effects acting as a secondary modifier of the primary signal.

4.2.3.3 Increase in the relative abundance of cyanobacteria with UV protection mechanisms

Since the 1970s, there has been an increase in the relative abundance of scytonemin, a pigment produced by cyanobacteria that provides effective protection against UV light (Garcia-Pichelt and Castenholz, 1993). Additionally, green algae contain zeaxanthin, a protective pigment against excessive radiation (Demmig-Adams and Adams, 2006), which has also increased modestly since the 1970s. Sierra Nevada experiences highest irradiances and daily doses of photosynthetically active radiation (PAR), UV-A, UV-B, (Monforte et al., 2015b, a), due to its high altitude and low latitude (Aphalo et al., 2012). Under this UV-stressful environment, algae typically develop repair mechanisms or photoprotective compounds (Demmig-Adams and Adams, 2006). Therefore, it is likely that these pigments have increased in response to higher UV radiation intensity. However, in Sierra Nevada, the reconstructed biologically effective UV-B (280-320 nm) did not show a clear increasing trend from 1913 to 2006 yr CE (Monforte et al., 2015b). Moreover, the period of increased scytonemin coincided with a rise in DOCw (Fig. 3), whose concentration is inversely related to water transparency (Morris et al., 1995).

It seems reasonable to suggest that the observed increase in scytonemin and zeaxanthin may be linked to the growth of cyanobacteria, Chlorophyceae and Zygnematophycea in radiation-exposed environments within the lake and associated wet alpine meadows (Hauer et al., 1997). These environments include planktonic, epiphytic and/or epilithic habitats and algal mats growing in shallow waters, where protection against UV radiation is crucial. This is supported by current observations of these algae in these areas.

In Borreguil Lake, where light penetrates the entire water column, green algae and cyanobacteria may outcompete diatoms due to their higher tolerance to UV light. Dense mats of benthic and littoral Zygnematophyceae may have limited diatom growth through shading and competition for space (DeNicola, 1996). These conditions of elevated temperature and UV exposure may have favoured green algae and cyanobacteria over diatoms.

5. Conclusions

This study provides novel evidence of ecological changes on a timescale of approximately ~400 years in a high-mountain lake ecosystem within Sierra Nevada National Park, highlighting the sensitivity of algal communities to both climatic variability

and atmospheric nutrient inputs. By integrating subfossil pigment analysis with regional climate reconstructions, our findings underscore the significant role of temperature, precipitation, and phosphorus deposition from Saharan dust in shaping primary producer dynamics.

Our paleolimnological analysis uncovered significant transformations in algal communities, marked fluctuations in chlorophyll-a concentrations, and notable shifts in geochemical proxies spanning the last ~400 years—with the most dramatic changes occurring over the past six decades. During this recent interval, algal biomass reached levels unprecedented in the four-century record, pointing to the intensified influence of climate warming and Saharan dust on Sierra Nevada lakes.

Two major ecological shifts, occurring around ~1840 CE and ~1970 CE, appear to reflect periods of intensified environmental forcing and marked ecosystem responses. The first coincided with the end of the Little Ice Age, signalling an early warming phase and an associated rise in algal productivity. The second, more pronounced shift, reflects the compounded impact of warmer and drier climate conditions and intensified dust-driven nutrient enrichment. This led to a fundamental restructuring of the algal community, with previously unseen abundances of N_2-fixing cyanobacteria, cryptophytes, and UV-resistant taxa, while diatoms declined.

The algal changes in this study align with global climate patterns and match the timing and direction of shifts in other alpine lakes. Our findings clarify the environmental preferences of key algal groups, helping us predict how algae will respond to future habitat changes. This is especially relevant given the projected increases in temperature, aridity, and nutrient inputs from Saharan dust in sensitive regions.

CRedIT authorship

Joana Llodrà-Llabrés: Writing - Original Draft, Conceptualization, Investigation - Data collection, Visualization; Carmen Pérez-Martínez: Writing - Review & Editing, Conceptualization, Investigation - Data collection, formal analysis; Supervision, financial; John P. Smol: Data collection, Writing - Review & Editing; Carsten Meyer-Jacob: Data collection, Writing - Review & Editing; Teresa Vegas: Conceptualization, Financial support, Review and Editing; Javier Sigro: writing - Review & Editing, Conceptualization, Investigation; Teresa Buchaca: Pigment analyses, writing - Review & Editing, Conceptualization, Investigation, Supervision.

Acknowledgements

This research is part of the project LACEN (OAPN 2403-S/2017) which has been co-funded by the Ministry of Ecological transition in their National Park Autonomous Agency (OAPN) action line. This work was partially funded by grant BIOD22_001, funded by Consejería de Universidad, Investigación e Innovación and Gobierno de España and Unión Europea – NextGenerationEU. This research is part of the project LifeWatch-2019-10-UGR-01, which has been co-funded by the Ministry of Science and Innovation through the FEDER funds from the Spanish Pluriregional Operational Program 2014-2020

(POPE), LifeWatch-ERIC action line. This work was supported by the Natural Sciences and Engineering Research Council of Canada.

JLL was funded by an Aid for University Teacher Training FPU 2019 (FPU19/04878) by the Spanish Ministry of Universities.

Data availability

The pigment, paleoenvironmental, and dating datasets, along with the statistical code used for RDA analysis, are openly available in the following GitHub repositories: https://github.com/carmen6363/Pigment-article-variables-2026, https://github.com/carmen6363/Dating-results-core-SSBG-21 and https://github.com/carmen6363/RDA-pigment.

References

Adrian, R., O'Reilly, C. M., Zagarese, H., Baines, S. B., Hessen, D. O., Keller, W., Livingstone, D. M., Sommaruga, R., Straile, D., Van Donk, E., Weyhenmeyer, G. A., and Winder, M.: Lakes as sentinels of climate change, Limnol. Oceanogr., 54, 2283–2297, https://doi.org/10.4319/lo.2009.54.6_part_2.2283, 2009.

Anderson, N., Odgaard, B., Segerström, U., and Renberg, I.: Climate-lake interactions recorded in varved sediments from a Swedish boreal forest lake, Glob. Chang. Biol., 2, 399–403, https://doi.org/10.1111/j.1365-2486.1996.tb00090.x, 1996.

Anderson, R. S., Jiménez-Moreno, G., Carrión, J. S., and Pérez-Martínez, C.: Postglacial history of alpine vegetation, fire, and climate from Laguna de Río Seco, Sierra Nevada, southern Spain, Quat. Sci. Rev., 30, 1615–1629, https://doi.org/10.1016/j.quascirev.2011.03.005, 2011.

Aphalo, P. J., Albert, A., Björn, L. O., Mcleod, A. R., Robson, T. M., and Rosenqvist, E.: Beyond the visible: A handbook of best practice in plant UV photobiology, edited by: Aphalo, P. J., Albert, A., Björn, L. O., Mcleod, A. R., Robson, T. M., and Rosenqvist, E., COST Action FA0906 UV4growth. Helsinki: University of Helsinki, Division of Plant Biology., 176 pp., 2012.

Appleby, P. G. and Oldfield, F.: The calculation of lead-210 dates assuming a constant rate of supply of unsupported 210Pb to the sediment, CATENA, 5, 1–8, https://doi.org/https://doi.org/10.1016/S0341-8162(78)80002-2, 1978.

Baron, J. S., Rueth, H. M., Wolfe, A. M., Nydick, K. R., Allstott, E. J., Minear, J. T., and Moraska, B.: Ecosystem responses to nitrogen deposition in the Colorado Front Range, Ecosystems, 3, 352–368, https://doi.org/10.1007/s100210000032, 2000.

Barone, R. and Naselli-Flores, L.: Distribution and seasonal dynamics of Cryptomonads in Sicilian water bodies, 2003.

Bartón, K.: MuMIn: Multi-Model Inference. R package version 1.48.11, https://CRAN.R-project.org/package=MuMIn, 2025.

Battarbee, R. W., Grytnes, J. A., Thompson, R., Appleby, P. G., Catalan, J., Korhola, A., Birks, H. J. B., Heegaard, E., and Lami, A.: Comparing palaeolimnological and instrumental evidence of climate change for remote mountain lakes over the last 200 years, J. Paleolimnol., 28, 161–179, https://doi.org/10.1023/A:1020384204940, 2002.

Becker, A., P. Finger, A. Meyer-Christoffer, B. Rudolf, K. Schamm, U. Schneider, and Ziese, M.: A description of the global land-surface precipitation data products of the Global Precipitation Climatology Centre with sample applications including centennial (trend) analysis from 1901-present. Earth Sys. Sci. Data, doi:10.5194/essd-5-71-2013, 2013.

Bennett, K. D.: Determination of the number of zones in a biostratigraphical sequence, New Phytol., 132, 155–170, https://doi.org/10.1111/j.1469-8137.1996.tb04521.x, 1996.

Bergström, A.-K. and Jansson, M.: Atmospheric nitrogen deposition has caused nitrogen enrichment and eutrophication of lakes in the northern hemisphere, Glob. Chang. Biol., 12, 635–643, https://doi.org/https://doi.org/10.1111/j.1365-2486.2006.01129.x, 2006.

Brahney, J., Ballantyne, A. P., Kociolek, P., Spaulding, S., Otu, M., Porwoll, T., and Neff, J. C.: Dust mediated transfer of phosphorus to alpine lake ecosystems of the Wind River Range, Wyoming, USA, Biogeochemistry, 120, 259–278, https://doi.org/10.1007/s10533-014-9994-x, 2014.

Brahney, J., Ballantyne, A. P., Kociolek, P., Leavitt, P. R., Farmer, G. L., and Neff, J. C.: Ecological changes in two contrasting lakes associated with human activity and dust transport in western Wyoming, Limnol. Oceanogr., 60, 678–695, https://doi.org/10.1002/lno.10050, 2015a.

Brahney, J., Mahowald, N., Ward, D. S., Ballantyne, A. P., and Neff, J. C.: Is atmospheric phosphorus pollution altering global alpine Lake stoichiometry?, Global Biogeochem. Cycles, 29, 1369–1383, https://doi.org/https://doi.org/10.1002/2015GB005137, 2015b.

Buchaca, T. and Catalan, J.: Factors influencing the variability of pigments in the surface sediments of mountain lakes, Freshw. Biol., 52, 1365–1379, https://doi.org/10.1111/j.1365-2427.2007.01774.x, 2007.

Buchaca, T. and Catalan, J.: On the contribution of phytoplankton and benthic biofilms to the sediment record of marker pigments in high mountain lakes, J. Paleolimnol., 40, 369–383, https://doi.org/10.1007/s10933-007-9167-1, 2008.

Buchaca, T. and Catalan, J.: Nonlinearities in phytoplankton groups across temperate high mountain lakes, J. Ecol., 112, 755–769, https://doi.org/10.1111/1365-2745.14267, 2024.

Buchaca, T., Felip, M., and Catalan, J.: A comparison of HPLC pigment analyses and biovolume estimates of phytoplankton

groups in an oligotrophic lake, J. Plankton Res., 27, 91–101, https://doi.org/10.1093/plankt/fbh154, 2005.

Buchaca, T., Kosten, S., Lacerot, G., Mazzeo, N., Kruk, C., Huszar, V. L. M., Lotter, A. F., and Jeppesen, E.: Pigments in surface sediments of South American shallow lakes as an integrative proxy for primary producers and their drivers, Freshw. Biol., 64, 1437–1452, https://doi.org/https://doi.org/10.1111/fwb.13317, 2019.

Burnham, K. and Anderson, D.: Model Selection and Multimodel Inference, A Pract. Information-theoretic Approach, https://doi.org/10.1007/978-0-387-22456-5_5, 2004.

Camarero, L. and Catalán, J.: Atmospheric phosphorus deposition may cause lakes to revert from phosphorus limitation back to nitrogen limitation., Nat. Commun., 3, 1118, https://doi.org/http://doi.org/10.1038/ncomms2125, 2012.

Carrillo, P., Cruz-Pizarro, L., and Morales-Baquero, R.: Effects of unpredictable atmospheric allochthonous input on the light climate of an oligotrophic lake, SIL Proceedings, 1922-2010, 24, 97–101, https://doi.org/10.1080/03680770.1989.11898698, 1990.

Castellano-Hinojosa, A., Correa-Galeote, D., Carrillo, P., Bedmar, E. J., and Medina-Sánchez, J. M.: Denitrification and biodiversity of denitrifiers in a High-Mountain Mediterranean Lake, Front. Microbiol., 8, 1911, https://doi.org/10.3389/fmicb.2017.01911, 2017.

Castillo Martín, A.: Lagunas de Sierra Nevada, ed, Univ. Granada, Granada, 2009.

Chiapello, I., Moulin, C., and Prospero, J. M.: Understanding the long-term variability of African dust transport across the Atlantic as recorded in both Barbados surface concentrations and large-scale Total Ozone Mapping Spectrometer (TOMS) optical thickness, J. Geophys. Res. Atmos., 110, https://doi.org/https://doi.org/10.1029/2004JD005132, 2005.

Cuesta Linares, E. J.: Las diatomeas bentónicas de las lagunas del Parque Nacional de Sierra Nevada. Estudio comparado con las colecciones del herbario de la Universidad de Granada (GDA), PhD thesis, Universidad de Granada, 2003.

Demmig-Adams, B. and Adams, W. W.: Photoprotection in an ecological context: The remarkable complexity of thermal energy dissipation, https://doi.org/10.1111/j.1469-8137.2006.01835.x, October 2006.

DeNicola, D. M.: 6 - Periphyton Responses to Temperature at Different Ecological Levels, in: Algal Ecology, edited by: Stevenson, R. J., Bothwell, M. L., and Lowe, R. L., Academic Press, San Diego, 149–181, https://doi.org/https://doi.org/10.1016/B978-012668450-6/50035-7, 1996.

Douglas, M. and Smol, J.: Freshwater diatoms as indicators of environmental change in the High Arctic, Diatoms Appl.

Environ. Earth Sci. Second Ed., 249–266, https://doi.org/10.1017/CBO9780511763175.014, 2010.

Dubois, N., Saulnier-Talbot, É., Mills, K., Gell, P., Battarbee, R., Bennion, H., Chawchai, S., Dong, X., Francus, P., Flower, R., Gomes, D. F., Gregory-Eaves, I., Humane, S., Kattel, G., Jenny, J. P., Langdon, P., Massaferro, J., McGowan, S., Mikomägi, A., Ngoc, N. T. M., Ratnayake, A. S., Reid, M., Rose, N., Saros, J., Schillereff, D., Tolotti, M., and Valero-Garcés, B.: First human impacts and responses of aquatic systems: A review of palaeolimnological records from around the world, Anthr. Rev., 5, 28–68, https://doi.org/10.1177/2053019617740365, 2018.

Elmslie, B. G., Gushulak, C. A. C., Boreux, M. P., Lamoureux, S. F., Leavitt, P. R., and Cumming, B. F.: Complex responses of phototrophic communities to climate warming during the Holocene of northeastern Ontario, Canada, Holocene, 30, 272–288, https://doi.org/10.1177/0959683619883014, 2020.

Engardt, M., Simpson, D., Schwikowski, M., and Granat, L.: Deposition of sulphur and nitrogen in Europe 1900–2050. Model calculations and comparison to historical observations, Tellus, Ser. B Chem. Phys. Meteorol., 69, https://doi.org/10.1080/16000889.2017.1328945, 2017.

Escudero, M., Castillo, S., Querol, X., Avila, A., Alarcón, M., Viana, M. M., Alastuey, A., Cuevas, E., and Rodríguez, S.: Wet and dry African dust episodes over eastern Spain, J. Geophys. Res. D Atmos., 110, 1–15, https://doi.org/10.1029/2004JD004731, 2005.

Florian, C. R., Miller, G. H., Fogel, M. L., Wolfe, A. P., Vinebrooke, R. D., and Geirsdóttir, Á.: Algal pigments in Arctic lake sediments record biogeochemical changes due to Holocene climate variability and anthropogenic global change, J. Paleolimnol., 54, 53–69, https://doi.org/10.1007/s10933-015-9835-5, 2015.

García-Alix, A., Jimenez-Espejo, F. J., Lozano, J. A., Jiménez-Moreno, G., Martinez-Ruiz, F., García Sanjuán, L., Aranda Jiménez, G., García Alfonso, E., Ruiz-Puertas, G., and Anderson, R. S.: Anthropogenic impact and lead pollution throughout the Holocene in Southern Iberia, Sci. Total Environ., 449, 451–460, https://doi.org/https://doi.org/10.1016/j.scitotenv.2013.01.081, 2013.

García-Alix, A., Toney, J. L., Jiménez-Moreno, G., Pérez-Martínez, C., Jiménez, L., Rodrigo-Gámiz, M., Scott Anderson, R., Camuera, J., Jiménez-Espejo, F. J., Peña-Angulo, D., and Ramos-Roman, M. J.: Algal lipids reveal unprecedented warming rates in alpine areas of SW Europe during the industrial period, Clim. Past, 16, 245–263, https://doi.org/10.5194/cp-16-245-2020, 2020.

Garcia-Pichelt, F. and Castenholz, R. W.: Occurrence of UV-Absorbing, Mycosporine-Like Compounds among Cyanobacterial Isolates and an Estimate of Their Screening Capacity, Appl. Environ. Microbiol., 163–169 pp., 1993.

Giorgi, F.: Climate change hot-spots, Geophys. Res. Lett., 33, https://doi.org/10.1029/2006GL025734, 2006.

Glew, J.R., Smol, J.P. and Last, W.M.: Sediment core collection and extrusion. pp. 73-105, in: Tracking Environmental Change Using Lake Sediments. Vol 1: Basin Analysis, Coring, and Chronological Techniques, edited by Last, W.M. and Smol, J.P., Kluwer Academic Publishers, Dordrecht, 2001.

González-Olalla, J. M. and Brahney, J.: Diverse dust sources and warming trigger cyanobacteria abundance in freshwater ecosystems in the western United States, Environ. Res., 278, 121663, https://doi.org/https://doi.org/10.1016/j.envres.2025.121663, 2025.

González-Olalla, J. M., Medina-Sánchez, J. M., Lozano, I. L., Villar-Argaiz, M., and Carrillo, P.: Climate-driven shifts in algal-bacterial interaction of high-mountain lakes in two years spanning a decade, Sci. Rep., 8, 10278, https://doi.org/10.1038/s41598-018-28543-2, 2018.

Grimm, E. C.: Tilia 1.7.16 Software. Illinois State Museum, Research and Collection Center: Springfield, IL, 2011.

Hauer, F. R., Baron, J. S., Campbell, D. H., Fausch, K. D., Hostetler, S. W., Leavesley, G. H., Leavitt, P. R., Mcknight, D. M., and Stanford, J. A.: Assessment of climate change and freshwater ecosystems of the Rocky Mountains, USA and Canada, Hydrol. Process., 11, 903–924, https://doi.org/10.1002/(sici)1099-1085(19970630)11:8<903::aid-hyp511>3.0.co;2-7, 1997.

Havens, K. E. and Paerl, H. W.: Climate Change at a Crossroad for Control of Harmful Algal Blooms, https://doi.org/10.1021/acs.est.5b03990, 3 November 2015.

Hofmann, A. M., Kuefner, W., Mayr, C., Dubois, N., Geist, J., and Raeder, U.: Unravelling climate change impacts from other anthropogenic influences in a subalpine lake: a multi-proxy sediment study from Oberer Soiernsee (Northern Alps, Germany), Hydrobiologia, 848, 4285–4309, https://doi.org/10.1007/s10750-021-04640-8, 2021.

Holland, E. A., Lee-Taylor, J., Nevison, C., and Sulzman, J. M.: Global N Cycle: Fluxes and N2O Mixing Ratios Originating from Human Activity, https://doi.org/10.3334/ORNLDAAC/797, 2005.

Holtgrieve, G. W., Schindler, D. E., Hobbs, W. O., Leavitt, P. R., Ward, E. J., Bunting, L., Chen, G., Finney, B. P., Gregory-Eaves, I., Holmgren, S., Lisac, M. J., Lisi, P. J., Nydick, K., Rogers, L. A., Saros, J. E., Selbie, D. T., Shapley, M. D., Walsh, P. B., and Wolfe, A. P.: A Coherent Signature of Anthropogenic Nitrogen Deposition to Remote Watersheds of the Northern Hemisphere, Science (80-.)., 334, 1545–1548, https://doi.org/10.1126/science.1212267, 2011.

Hu, Z., Anderson, N. J., Yang, X., and Mcgowan, S.: Catchment-mediated atmospheric nitrogen deposition drives ecological change in two alpine lakes in SE Tibet, Glob. Chang. Biol., 20, 1614–1628, https://doi.org/10.1111/gcb.12435, 2014.

762 Huo, S., Zhang, H., Wang, J., Chen, J., and Wu, F.: Temperature and precipitation dominates millennium changes of eukaryotic
763 algal communities in Lake Yamzhog Yumco, Southern Tibetan Plateau, Sci. Total Environ., 829,
764 https://doi.org/10.1016/j.scitotenv.2022.154636, 2022.

765 Hurrell, J. W.: Decadal Trends in the North Atlantic Oscillation: Regional Temperatures and Precipitation, Science (80-.)..,
766 269, 676–679, https://doi.org/10.1126/science.269.5224.676, 1995.

767 IPCC: High Mountain Areas, in: The Ocean and Cryosphere in a Changing Climate, Cambridge University Press, 131–202,
768 https://doi.org/10.1017/9781009157964.004, 2022.

769 Jeffrey, S. W., Mantoura, R. F. C., and Wright, S. W.: Phytoplankton pigments in oceanography: guidelines to modern
770 methods. 661p. Paris: Unesco Publishing, 1997. (Monographs on Oceanographic Methodology no. 10)., 2009/05/11.,
771 Cambridge University Press, 918 pp., https://doi.org/DOI: 10.1017/S0025315400036389, 1997.

772 Jiménez-Espejo, F. J., García-Alix, A., Jiménez-Moreno, G., Rodrigo-Gámiz, M., Anderson, R. S., Rodríguez-Tovar, F. J.,
773 Martínez-Ruiz, F., Giralt, S., Delgado Huertas, A., and Pardo-Igúzquiza, E.: Saharan aeolian input and effective humidity
774 variations over western Europe during the Holocene from a high altitude record, Chem. Geol., 374–375, 1–12,
775 https://doi.org/10.1016/j.chemgeo.2014.03.001, 2014.

776 Jiménez-Moreno, G., García-Alix, A., Anderson, R. S., Ramos-Román, M. J., Camuera, J., Mesa-Fernández, J. M., Toney, J.
777 L., Jiménez-Espejo, F. J., Carrión, J. S., López-Avilés, A., Rodrigo-Gámiz, M., and Webster, C. E.: Reconstruction of Past
778 Environment and Climate Using Wetland Sediment Records from the Sierra Nevada, in: The Landscape of the Sierra Nevada:
779 A Unique Laboratory of Global Processes in Spain, edited by: Zamora, R. and Oliva, M., Springer International Publishing,
780 Cham, 95–114, https://doi.org/10.1007/978-3-030-94219-9_7, 2022.

781 Jiménez-Moreno, G., Heiri, O., García-Alix, A., Anderson, R. S., Jiménez-Espejo, F. J., López-Blanco, C., Jiménez, L., Pérez-
782 Martínez, C., Rodrigo-Gámiz, M., López-Avilés, A., and Camuera, J.: Holocene summer temperature reconstruction based on
783 a chironomid record from Sierra Nevada, southern Spain, Quat. Sci. Rev., 319,
784 https://doi.org/10.1016/j.quascirev.2023.108343, 2023.

785 Jiménez, Laura, Romero-Viana, Lidia, Conde-Porcuna, José María, and Pérez-Martínez, Carmen: Sedimentary photosynthetic
786 pigments as indicators of climate and watershed perturbations in an alpine lake in southern Spain, Limnetica, 439–454,
787 https://doi.org/10.23818/limn.34.33, 2015.

788 Jiménez, L., Rühland, K. M., Jeziorski, A., Smol, J. P., and Pérez-Martínez, C.: Climate change and Saharan dust drive recent
789 cladoceran and primary production changes in remote alpine lakes of Sierra Nevada, Spain, Glob. Chang. Biol., 24, e139–

e158, https://doi.org/10.1111/gcb.13878, 2018.

Jiménez, L., Conde-Porcuna, J. M., García-Alix, A., Toney, J. L., Anderson, R. S., Heiri, O., and Pérez-Martínez, C.: Ecosystem Responses to Climate-Related Changes in a Mediterranean Alpine Environment Over the Last ~ 180 Years, Ecosystems, 22, 563–577, https://doi.org/10.1007/s10021-018-0286-5, 2019.

Korbee, N., Carrillo, P., Mata, M. T., Rosillo, S., Medina-Sánchez, J. M., and Figueroa, F. L.: Effects of ultraviolet radiation and nutrients on the structure-function of phytoplankton in a high mountain lake, Photochem. Photobiol. Sci., 11, 1087–1098, https://doi.org/10.1039/c2pp05336e, 2012.

Lami, A., Turner, S., Musazzi, S., Gerli, S., Guilizzoni, P., Rose, N. L., Yang, H., Wu, G., and Yang, R.: Sedimentary evidence for recent increases in production in Tibetan plateau lakes, Hydrobiologia, 648, 175–187, https://doi.org/10.1007/s10750-010-0263-2, 2010.

Laurion, I., Ventura, M., Catalan, J., Psenner, R., & Sommaruga, R.: Attenuation of ultraviolet radiation in mountain lakes: factors controlling the among-and within-lake variability. Limnol. Oceanogr., 45(6), 1274-1288, https://doi.org/10.4319/lo.2000.45.6.1274, 2000.

Leavitt, P. R. and Hodgson, D. A.: Sedimentary Pigments, in: Tracking Environmental Change Using Lake Sediments: Terrestrial, Algal, and Siliceous Indicators, edited by: Smol, J. P., Birks, H. J. B., Last, W. M., Bradley, R. S., and Alverson, K., Springer Netherlands, Dordrecht, 295–325, https://doi.org/10.1007/0-306-47668-1_15, 2001.

Legendre, P. and Birks, H. J. B.: Clustering and Partitioning, in Tracking Environmental Change Using Lake Sediments: Data Handling and Numerical Techniques, edited by: Birks, H. J. B., Lotter, A. F., Juggins, S., and Smol, J. P., Springer Netherlands, Dordrecht, 167–200, https://doi.org/10.1007/978-94-007-2745-8_7, 2012.

López-Merino, L., Moreno, A., Leira, M., Sigró, J., González-Sampériz, P., Valero-Garcés, B. L., López-Sáez, J. A., Brunet, M., and Aguilar, E.: Two hundred years of environmental change in Picos de Europa National Park inferred from sediments of Lago Enol, northern Iberia, J. Paleolimnol., 46, 453–467, https://doi.org/10.1007/s10933-011-9546-5, 2011.

Mackey, M. D., Mackey, D. J., Higgins, H. W., and Wright, S. W.: CHEMTAX - a program for estimating class abundances from chemical markers: application to HPLC measurements of phytoplankton, Mar. Ecol. Prog. Ser., 144, 265–283, 1996.

Medina-Sánchez, J. M., Cabrerizo, M. J., González-Olalla, J. M., Villar-Argaiz, M., & Carrillo, P.: High mountain lakes as remote sensors of global change, in: The Landscape of the Sierra Nevada: A Unique Laboratory of Global Processes in Spain, edited by: Zamora, R. and Oliva, M., Springer International Publishing, Cham, 261-278, https://doi.org/10.1007/978-3-030-

94219-9_16, 2022.

Meyer-Jacob, C., Michelutti, N., Paterson, A. M., Monteith, D., Yang, H., Weckström, J., Smol, J. P., and Bindler, R.: Inferring Past Trends in Lake Water Organic Carbon Concentrations in Northern Lakes Using Sediment Spectroscopy, Environ. Sci. Technol., 51, 13248–13255, https://doi.org/10.1021/acs.est.7b03147, 2017.

Meyer-Jacob, C., Michelutti, N., Paterson, A. M., Cumming, B. F., Keller, W., and Smol, J. P.: The browning and re-browning of lakes: Divergent lake-water organic carbon trends linked to acid deposition and climate change, Sci. Rep., 9, https://doi.org/10.1038/s41598-019-52912-0, 2019.

Meyers, P. A. and Teranes, J. L.: Sediment Organic Matter, in Tracking Environmental Change Using Lake Sediments: Physical and Geochemical Methods, edited by: Last, W. M. and Smol, J. P., Springer Netherlands, Dordrecht, 239–269, https://doi.org/10.1007/0-306-47670-3_9, 2001.

Michelutti, N., and Smol, J. P.: Visible spectroscopy reliably tracks trends in paleo-production, J. Paleolimnol., 56, 253–265, https://doi.org/10.1007/s10933-016-9921-3, 2016.

Michelutti, N., Wolfe, A. P., Vinebrooke, R. D., Rivard, B., and Briner, J. P.: Recent primary production increases in arctic lakes, Geophys. Res. Lett., 32, 1–4, https://doi.org/10.1029/2005GL023693, 2005.

Michelutti, N., Blais, J. M., Cumming, B. F., Paterson, A. M., Rühland, K., Wolfe, A. P., and Smol, J. P.: Do spectrally inferred determinations of chlorophyll a reflect trends in lake trophic status?, J. Paleolimnol., 43, 205–217, https://doi.org/10.1007/s10933-009-9325-8, 2010.

Mladenov, N., Pulido-Villena, E., Morales-Baquero, R., Ortega-Retuerta, E., Sommaruga, R., and Reche, I.: Spatiotemporal drivers of dissolved organic matter in high alpine lakes: Role of Saharan dust inputs and bacterial activity, J. Geophys. Res. Biogeosciences, 113, https://doi.org/https://doi.org/10.1029/2008JG000699, 2008.

Mladenov, N., López-Ramos, J., McKnight, D. M., and Reche, I.: Alpine lake optical properties as sentinels of dust deposition and global change, Limnol. Oceanogr., 54, 2386–2400, https://doi.org/10.4319/lo.2009.54.6_part_2.2386, 2009.

Monforte, L., Tomás-Las-Heras, R., Del-Castillo-Alonso, M. Á., Martínez-Abaigar, J., and Núñez-Olivera, E.: Spatial variability of ultraviolet-absorbing compounds in an aquatic liverwort and their usefulness as biomarkers of current and past UV radiation: A case study in the Atlantic-Mediterranean transition, Sci. Total Environ., 518–519, 248–257, https://doi.org/10.1016/j.scitotenv.2015.03.006, 2015a.

Monforte, L., Núñez-Olivera, E., and Martínez-Abaigar, J.: UV radiation biomonitoring using cell compartmentation of UV-

absorbing compounds in herbarium samples of a liverwort, Ecol. Indic., 52, 48–56, https://doi.org/10.1016/j.ecolind.2014.11.027, 2015b.

Morales-Baquero, R. and Pérez-Martínez, C.: Saharan versus local influence on atmospheric aerosol deposition in the southern Iberian Peninsula: Significance for N and P inputs, Global Biogeochem. Cycles, 30, 501–513, https://doi.org/https://doi.org/10.1002/2015GB005254, 2016.

Morales-Baquero, R., Carrillo, P., Reche, I., and Sánchez-Castillo, P.: Nitrogen-phosphorus relationship in high mountain lakes: effects of the size of catchment basins, Can. J. Fish. Aquat. Sci., 56, 1809–1817, https://doi.org/10.1139/f99-130, 1999.

Morales-Baquero, R., Carrillo, P., Barea-Arco, J., Pérez-Martínez, C., and Villar-Argaiz, M.: Climate-driven changes on phytoplankton–zooplankton coupling and nutrient availability in high mountain lakes of Southern Europe, Freshw. Biol., 51, 989–998, https://doi.org/10.1111/j.1365-2427.2006.01545.x, 2006a.

Morales-Baquero, R., Pulido-Villena, E., & Reche, I.: Atmospheric inputs of phosphorus and nitrogen to the southwest Mediterranean region: Biogeochemical responses of high mountain lakes. *Limnology and Oceanography*, *51*(2), 830-837, https://doi.org/10.4319/lo.2006.51.2.0830, 2006b.

Morales-Baquero, R., Pulido-Villena, E., and Reche, I.: Chemical signature of saharan dust on dry and wet atmospheric deposition in the south-western mediterranean region, Tellus, Ser. B Chem. Phys. Meteorol., 65, https://doi.org/10.3402/tellusb.v65i0.18720, 2013.

Morris, D. P., Zagarese, H., Williamson, C. E., Balseiro, E. G., Hargreaves, B. R., Modenutti, B., Moeller, R., and Queimalinos, C.: The attenuation of solar UV radiation in lakes and the role of dissolved organic carbon, Limnol. Oceanogr., 40, 1381–1391, https://doi.org/10.4319/lo.1995.40.8.1381, 1995.

Moser, K. A., Baron, J. S., Brahney, J., Oleksy, I. A., Saros, J. E., Hundey, E. J., Sadro, S. A., Kopáček, J., Sommaruga, R., Kainz, M. J., Strecker, A. L., Chandra, S., Walters, D. M., Preston, D. L., Michelutti, N., Lepori, F., Spaulding, S. A., Christianson, K. R., Melack, J. M., and Smol, J. P.: Mountain lakes: Eyes on global environmental change, Glob. Planet. Change, 178, 77–95, https://doi.org/10.1016/j.gloplacha.2019.04.001, 2019.

Moulin, C. and Chiapello, I.: Evidence of the control of summer atmospheric transport of African dust over the Atlantic by Sahel sources from TOMS satellites (1979–2000), Geophys. Res. Lett., 31, https://doi.org/https://doi.org/10.1029/2003GL018931, 2004.

Moulin, C. and Chiapello, I.: Impact of human-induced desertification on the intensification of Sahel dust emission and export

over the last decades, Geophys. Res. Lett., 33, https://doi.org/https://doi.org/10.1029/2006GL025923, 2006.

Moulin, C., Lambert, C. E., Dulac, F., and Dayan, U.: Control of atmospheric export of dust from North Africa by the North Atlantic Oscillation, Nature, 387, 691–694, https://doi.org/10.1038/42679, 1997.

Mulitza, S., Heslop, D., Pittauerova, D., Fischer, H. W., Meyer, I., Stuut, J.-B., Zabel, M., Mollenhauer, G., Collins, J. A., Kuhnert, H., and Schulz, M.: Increase in African dust flux at the onset of commercial agriculture in the Sahel region., Nature, 466, 226–228, https://doi.org/10.1038/nature09213, 2010.

Nogués-Bravo, D., Araújo, M. B., Lasanta, T., and Moreno, J. I. L.: Climate change in Mediterranean mountains during the 21st century, Ambio, 37, 280–285, https://doi.org/10.1579/0044-7447(2008)37[280:CCIMMD]2.0.CO;2, 2008.

Oksanen, J., Simpson, G. L., Blanchet, F. G., Kindt, R., Legendre, P., Minchin, P. R., ... and Weedon, J.: Vegan: Community Ecology Package, 2022, https://cran.r-project.org/package=vegan, 2022.

Oleksy, I. A., Baron, J. S., Leavitt, P. R., and Spaulding, S. A.: Nutrients and warming interact to force mountain lakes into unprecedented ecological states, Proc. R. Soc. Lond. B Biol. Sci., 287 (1930), https://doi.org/10.1098/rspb.2020.0304, 2020.

Oleksy, I. A., Collins, S. M., Sillen, S. J., Topp, S. N., Austin, M., Hall, E. K., O'Reilly, C. M., Yang, X., and Ross, M. R. V: Heterogenous controls on lake color and trends across the high-elevation U.S. Rocky Mountain region, Environ. Res. Lett., 17, 104041, https://doi.org/10.1088/1748-9326/ac939c, 2022.

Oliva, M., Ruiz-Fernández, J., Barriendos, M., Benito, G., Cuadrat, J. M., Domínguez-Castro, F., García-Ruiz, J.M., Giralt, S., Gómez-Ortiz, A., Hernández, A., López-Costas, O., López-Moreno, J.I., López-Sáez, J.A., Martínez-Cortizas, A., Moreno, A., Prohom, M., Saz, M.A., Serrano, E., Tejedor, E., Trigo, R., Valero-Garcés, B., and Vicente-Serrano, S. M.: The Little Ice Age in Iberian mountains. Earth-Sci. Rev., 177, 175-208, https://doi.org/10.1016/j.earscirev.2017.11.010, 2018.

Pardo-Igúzquiza, E., Martos-Rosillo, S., Jódar, J., and Dowd, P. A.: The Spatio-Temporal Dynamics of Water Resources (Rainfall and Snow) in the Sierra Nevada Mountain Range (Southern Spain), Resources, 13, https://doi.org/10.3390/resources13030042, 2024.

Pepin, N., Bradley, R. S., Diaz, H. F., Baraer, M., Caceres, E. B., Forsythe, N., Fowler, H., Greenwood, G., Hashmi, M. Z., Liu, X. D., Miller, J. R., Ning, L., Ohmura, A., Palazzi, E., Rangwala, I., Schöner, W., Severskiy, I., Shahgedanova, M., Wang, M. B., Williamson, S. N., and Yang, D. Q.: Elevation-dependent warming in mountain regions of the world, Nat. Clim. Chang., 5, 424–430, https://doi.org/10.1038/nclimate2563, 2015.

Pérez-Luque, A. J., Sánchez-Rojas, C. P., Zamora, R., Pérez-Pérez, R., & Bonet, F. J.: Dataset of Phenology of Mediterranean

high-mountain meadows flora (Sierra Nevada, Spain). PhytoKeys, (46), 89, https://doi.org/10.3897/phytokeys.46.9116, 2015.

Pérez-Martínez, C., Barea-Arco, J., Conde-Porcuna, J. M., and Morales-Baquero, R.: Reproduction strategies of Daphnia pulicaria population in a high mountain lake of Southern Spain, in: Hydrobiologia, 75–82, https://doi.org/10.1007/s10750-007-9084-3, 2007.

Pérez-Martínez, C., Conde-Porcuna, J. M., Moreno, E., Ramos-Rodríguez, E., and Jiménez, L.: Cladoceran assemblage distribution in shallow alpine lakes of Sierra Nevada (Spain) and its relationship with environmental variables, Aquat. Sci., 82, 1–13, https://doi.org/10.1007/s00027-019-0677-5, 2020a.

Pérez-Martínez, C., Rühland, K. M., Smol, J. P., Jones, V. J., and Conde-Porcuna, J. M.: Long-term ecological changes in Mediterranean mountain lakes linked to recent climate change and Saharan dust deposition revealed by diatom analyses, Sci. Total Environ., 727, 138519, https://doi.org/10.1016/j.scitotenv.2020.138519, 2020b.

Pérez-Martínez, C., Conde-Porcuna, J. M., Ramos-Rodríguez, E., Moreno, E., Rühland, K. M., Jeziorski, A., Smol, J. P., García-Alix, A., Heiri, O., Corral-Arredondo, E., and Jiménez, L.: Paleolimnological Indicators of Global Change, in: The Landscape of the Sierra Nevada: A Unique Laboratory of Global Processes in Spain, edited by: Zamora, R. and Oliva, M., Springer International Publishing, Cham, 279–291, https://doi.org/10.1007/978-3-030-94219-9_17, 2022.

Preston, D. L., Caine, N., McKnight, D. M., Williams, M. W., Hell, K., Miller, M. P., Hart, S. J., and Johnson, P. T. J.: Climate regulates alpine lake ice cover phenology and aquatic ecosystem structure, Geophys. Res. Lett., 43, 5353–5360, https://doi.org/10.1002/2016GL069036, 2016.

Preunkert, S. and Legrand, M.: Towards a quasi-complete reconstruction of past atmospheric aerosol load and composition (organic and inorganic) over Europe since 1920 inferred from Alpine ice cores, Clim. Past, 9, 1403–1416, https://doi.org/10.5194/cp-9-1403-2013, 2013.

Prospero, J. M. and Lamb, P. J.: African Droughts and Dust Transport to the Caribbean: Climate Change Implications, Science (80-.)., 302, 1024–1027, https://doi.org/10.1126/science.1089915, 2003.

Pulido-Villena, E., Reche, I., and Morales-Baquero, R.: Significance of atmospheric inputs of calcium over the southwestern Mediterranean region: High Mountain lakes as tools for detection, Global Biogeochem. Cycles, 20, https://doi.org/10.1029/2005GB002662, 2006.

Riegman, R. and Kraay, G. W.: Phytoplankton community structure derived from HPLC analysis of pigments in the Faroe-Shetland Channel during summer 1999: the distribution of taxonomic groups in relation to physical/chemical conditions in the

photic zone, J. Plankton Res., 23, 191–205, https://doi.org/10.1093/plankt/23.2.191, 2001.

Rogora, M., Frate, L., Carranza, M. L., Freppaz, M., Stanisci, A., Bertani, I., Bottarin, R., Brambilla, A., Canullo, R., Carbognani, M., Cerrato, C., Chelli, S., Cremonese, E., Cutini, M., Di Musciano, M., Erschbamer, B., Godone, D., Iocchi, M., Isabellon, M., Magnani, A., Mazzola, L., Morra di Cella, U., Pauli, H., Petey, M., Petriccione, B., Porro, F., Psenner, R., Rossetti, G., Scotti, A., Sommaruga, R., Tappeiner, U., Theurillat, J.-P., Tomaselli, M., Viglietti, D., Viterbi, R., Vittoz, P., Winkler, M., and Matteucci, G.: Assessment of climate change effects on mountain ecosystems through a cross-site analysis in the Alps and Apennines, Sci. Total Environ., 624, 1429–1442, https://doi.org/https://doi.org/10.1016/j.scitotenv.2017.12.155, 2018.

Rühland, K., Paterson, A. M., and Smol, J.: Hemispheric-scale patterns of climate-related shifts in planktonic diatoms from North America and European lakes, Glob. Chang. Biol., 14, 2740–2754, https://doi.org/10.1111/j.1365-2486.2008.01670.x, 2008.

Rühland, K. M., Paterson, A. M., and Smol, J. P.: Lake diatom responses to warming: reviewing the evidence, J. Paleolimnol., 54, https://doi.org/10.1007/s10933-015-9837-3, 2015.

Salvador, P., Pey, J., Pérez, N., Querol, X., and Artíñano, B.: Increasing atmospheric dust transport towards the western Mediterranean over 1948–2020, npj Clim. Atmos. Sci., 5, 34, https://doi.org/10.1038/s41612-022-00256-4, 2022.

Sánchez Castillo, P. M. and Morales Torres, M. C.: Algunas especies hidrofíticas de la provincia de Granada, An. del Jardín Botánico Madrid, 37, 677–692, 1980.

Saros, J. E., Michel, T. J., Interlandi, S. J., and Wolfe, A. P.: Resource requirements of Asterionella formosa and Fragilaria crotonensis in oligotrophic alpine lakes: Implications for recent phytoplankton community reorganizations, Can. J. Fish. Aquat. Sci., 62, 1681–1690, https://doi.org/10.1139/f05-077, 2005.

Saros, J. E., Clow, D. W., Blett, T., and Wolfe, A. P.: Critical nitrogen deposition loads in high-elevation lakes of the western US inferred from paleolimnological records, Water. Air. Soil Pollut., 216, 193–202, https://doi.org/10.1007/s11270-010-0526-6, 2011.

Schlüter, L., Lauridsen, T. L., Krogh, G., and Jørgensen, T.: Identification and quantification of phytoplankton groups in lakes using new pigment ratios – a comparison between pigment analysis by HPLC and microscopy, Freshw. Biol., 51, 1474–1485, https://doi.org/https://doi.org/10.1111/j.1365-2427.2006.01582.x, 2006.

Scholz, J. and Brahney, J.: Evidence for multiple potential drivers of increased phosphorus in high-elevation lakes, Sci. Total

Environ., 825, 153939, https://doi.org/https://doi.org/10.1016/j.scitotenv.2022.153939, 2022.

Schouten, S. J., Schmidhauser, N. R. M. M., Grosjean, M., Lami, A., Boltshauser-Kaltenrieder, P., van Leeuwen, J. F. N., Vogel, H., and Zahajská, P.: Lake anoxia, primary production, and algal community shifts in response to rapid climate changes during the Late Glacial, Biogeosciences, 22, 3821–3842, https://doi.org/10.5194/bg-22-3821-2025, 2025.

Sigro, J., Cisneros, M., Perez-Luque, A. J., Perez-Martinez, C., and Vegas-Vilarrubia, T.: Trends in temperature and precipitation at high and low elevations in the main mountain ranges of the Iberian Peninsula (1894–2020): The Sierra Nevada and the Pyrenees, Int. J. Climatol., 44, 2897–2920, https://doi.org/10.1002/joc.8487, 2024.

Sommaruga-Wögrath, S., Koinig, K. A., Schmidt, R., Sommaruga, R., Tessadri, R., and Psenner, R.: Temperature effects on the acidity of remote alpine lakes, Nature, 387, 64–67, 1997.

Sorvari, S. and Korhola, A.: Recent diatom assemblage changes in subarctic Lake Saanajärvi, NW Finnish Lapland, and their paleoenvironmental implications, Journal of Paleolimnology, 205 pp., 1998.

Spaulding, S. A., Otu, M. K., Wolfe, A. P., and Baron, J. S.: Paleolimnological Records of Nitrogen Deposition in Shallow, High-Elevation Lakes of Grand Teton National Park, Wyoming, U.S.A., Arctic, Antarct. Alp. Res., 47, 703–717, https://doi.org/10.1657/AAAR0015-008, 2015.

Steffen, W., Crutzen, P. J., and Mcneill, J. R.: The Anthropocene: Are Humans Now Overwhelming the Great Forces of Nature?, 614–621 pp., 2007.

Talbot, M. R.: Nitrogen Isotopes in Palaeolimnology, in: Tracking Environmental Change Using Lake Sediments: Physical and Geochemical Methods, edited by: Last, W. M. and Smol, J. P., Springer Netherlands, Dordrecht, 401–439, https://doi.org/10.1007/0-306-47670-3_15, 2001.

Taranu, Z. E., Gregory-Eaves, I., Leavitt, P. R., Bunting, L., Buchaca, T., Catalan, J., Domaizon, I., Guilizzoni, P., Lami, A., Mcgowan, S., Moorhouse, H., Morabito, G., Pick, F. R., Stevenson, M. A., Thompson, P. L., and Vinebrooke, R. D.: Acceleration of cyanobacterial dominance in north temperate-subarctic lakes during the Anthropocene, Ecol. Lett., 18, 375–384, https://doi.org/10.1111/ele.12420, 2015.

Tuccillo, M. T., Garla, S. C., Osburn, M. R., Nash, B. C., and Axford, Y.: Sedimentary pigments reveal complex ecosystem responses of primary producers to mid-Holocene summer anoxia in a small Greenland lake, Quaternary Science Reviews, 369, 109630, https://doi.org/10.1016/j.quascirev.2025.109630, 2025.

Williamson, C. E., Overholt, E. P., Brentrup, J. A., Pilla, R. M., Leach, T. H., Schladow, S. G., Warren, J. D., Urmy, S. S.,

Sadro, S., Chandra, S., and Neale, P. J.: Sentinel responses to droughts, wildfires, and floods: Effects of UV radiation on lakes and their ecosystem services, Front. Ecol. Environ., 14, 102–109, https://doi.org/10.1002/fee.1228, 2016.

Wolfe, A. P., Van Gorp, A. C., and Baron, J. S.: Recent ecological and biogeochemical changes in alpine lakes of Rocky Mountain National Park (Colorado, USA): A response to anthropogenic nitrogen deposition, Geobiology, 1, 153–168, https://doi.org/10.1046/j.1472-4669.2003.00012.x, 2003.

Yang, J.-R., Pick, F. R., and Hamilton, P. B.: Changes in the planktonic diatom flora of a large mountain lake in response to fertilization, J. Phycol., 32, 232–243, https://doi.org/https://doi.org/10.1111/j.0022-3646.1996.00232.x, 1996.

Zamora, R. and Oliva, M.: The Landscape of the Sierra Nevada, https://doi.org/10.1007/978-3-030-94219-9, 2022.

Zeng, L., Panizzo, V. N., Wang, Z., Huang, X., Chen, X., and McGowan, S.: Hydrological isolation accelerates algal blooms in floodplain lakes: Biomarker evidence from Dongting Lake, China and its satellite lake, Water Research, 279, 123430, https://doi.org/10.1016/j.watres.2025.123430, 2025.

Zhang, H., Huo, S., Yeager, K. M., He, Z., Xi, B., Li, X., Ma, C., and Wu, F.: Phytoplankton response to climate changes and anthropogenic activities recorded by sedimentary pigments in a shallow eutrophied lake, Sci. Total Environ., 647, 1398–1409, https://doi.org/10.1016/j.scitotenv.2018.08.081, 2019.

Zufiaurre, A., Felip, M., Giménez-Grau, P., Pla-Rabès, S., Camarero, L., and Catalan, J.: Episodic nutrient enrichments stabilise protist coexistence in planktonic oligotrophic conditions, J. Ecol., 109, 1717–1729, https://doi.org/10.1111/1365-2745.13591, 2021.